Title

AN INVESTIGATION OF HYDROSTATIC EXTRUSION AND OTHER DEFORMATION MODES FOR THE FABRICATION OF MULTI-FILAMENTARY NIOBIUM-TIN SUPERCONDUCTORS BY A POWDER METALLURGY APPROACH

Author

MacLeod, G.E.

Publication Date

1977-06-01

AN INVESTIGATION OF HYDROSTATIC EXTRUSION AND OTHER DEFORMATION MODES FOR THE FABRICATION OF MULTIFILAMENTARY NIOBIUM-TIN SUPERCONDUCTORS BY A POWDER METALLURGY APPROACH

Glen Earl MacLeod
(M. S. thesis)

June 1977

Prepared for the U. S. Energy Research and Development Administration under Contract W-7405-ENG-48

LBL-6622

An Investigation of Hydrostatic Extrusion and Other Deformation Modes for the Fabrication of Multifilamentary Niobium-Tin Superconductors by a Powder Metallurgy Approach

By

Glen Earl MacLeod

(M. S. Thesis)

June, 1977

LBL-6622

An Investigation of Hydrostatic Extrusion and Other Deformation Modes for the Fabrication of Multifilamentary Niobium-Tin Superconductors by a Powder Metallurgy Approach

TABLE OF CONTENTS

	Page Numbers
ABSTRACT	1
INTRODUCTION	2-4
EXPERIMENTAL PROCEDURE:	
I. Processing of the Wire	4-5
II. Analytical Techniques	6-7
RESULTS AND DISCUSSION:	
Conductor Length Requirements	7
Compact Processing	7-10
Hydrostatic Extrusion	10-13
CONCLUSIONS	13-14
ACKNOWLEDGEMENT	14-15
APPENDIX	16
REFERENCES:	
1 through 15	17
16 through 28	18
TABLE 1	19
FIGURE CAPTIONS:	
1 through 9	20
10 through 29	21
30 through 32	22
FIGURES	23-

AN INVESTIGATION OF HYDROSTATIC EXTRUSION AND OTHER DEFORMATION MODES FOR THE FABRICATION OF MULTIFILAMENTARY NIOBIUM-TIN SUPERCONDUCTORS BY A POWDER METALLURGY APPROACH

Glen Earl MacLeod

Materials and Molecular Research Division
Lawrence Berkeley Laboratory
and

Department of Mechanical Engineering
University of California
Berkeley, California 94720

ABSTRACT

Various aspects of a powder metallurgy approach to fabricate filamentary niobium-tin superconducting wire were investigated. Difficulties occurred due to lack of complete tin infiltration of the sintered niobium rod, formation of intermetallics during infiltration, and both cladding and core fracture during mechanical reduction. The influence of sintering time, infiltration temperature, and deformation mode was investigated. Progress is reported on the clarification of the role of several of the important process parameters.

INTRODUCTION

In 1911, H. Kamerlingh Onnes[1] observed that mercury lost all electrical resistance at 4.2°K. This phenomenon became known as superconductivity. During the next fifty years, little research was done in the area of superconductivity because no known superconductors had practical application. Then in 1961, Kunzler, et al.,[2] discovered that Nb_3Sn remained superconductive in high magnetic fields--the first superconductor found to do so.

Extensive work has since been done in the area of superconductor fabrication. Many of the high field superconductors, particularly those having the A15 structure, like Nb_3Sn, are inherently brittle and must be subjected to special fabricating processes to make them useable. Neither the Bell Telephone process[2] or the General Electric tape process,[3] two of the first successful fabrication processes developed, produced multifilamentary conductors.

Multifilamentary wire was developed by Tachikawa[4] in Japan in 1967, and has since been studied extensively in this country by Suenage, et al.,[5,6] working at Brookhaven National Laboratory. Tachikawa's original process and its modifications have become known as the "bronze process". The bronze process has found commercial acceptance due to the relative flexibility and intrinsic stability of the wire. This stability is due to the multifilamentary morphology of the wire and is described by Wilson, et al.[7]

At the Lawrence Berkeley Laboratory, multifilamentary Nb_3Sn superconducting tape and wire have been made using a unique powder metallurgy approach to fabrication.[8] Babu,[9] Garrett,[10] and Hemachalam[11] have optimized the process parameters and characterized the resulting tape. Since multifilamentary tape is less stable than multifilamentary wire, the tape process was modified to produce wire. Hemachalam[12] was able to fabricate Nb_3Sn superconducting wire that had a higher current density at high fields than commercially available wire. Hemachalam began with 0.19 in. rods and was only able to make 20 foot lengths.

One objective of this work was to scale up the existing powder metallurgy process in order to make long lengths of Nb_3Sn superconducting wire (a few hundred feet). The ability to make long lengths of wire would demonstrate the practical feasibility of the process and with long lengths of wire a superconducting solenoid could be made and tested.

It was originally envisioned that the powder metallurgy process could be directly scaled up by simply increasing the billet diameter (the billet length is fixed due to the furnace geometry) and leaving other process parameters the same. However, core and cladding fracture during wire drawing have now indicated that the process parameters must be re-evaluated.

The effects of sintering time and infiltration temperature were investigated. Hydrostatic extrusion was used as an alternative to form rolling and wire drawing. The nominal diameters of the infiltrated cores employed in this work were 1/2 in. and 3/4 in. as contrasted with the 3/16 in. cores used by Hemachalam.

EXPERIMENTAL PROCEDURE

I. Processing of the Wire

The powder metallurgy process requires six steps to go from a powder to the final superconducting wire. These steps are: 1) isostatic compaction of the niobium powder to impart the required porosity and green strength; 2) sintering of the niobium rod to give it strength and ductility; 3) infiltration of the rod with tin, thereby filling the pores with an inter-connected network of tin; 4) cladding of the rod to facilitate mechanical deformation; 5) mechanical reduction of the rod to produce a multifilamentary structure of tin in the niobium, and 6) diffusion treatment to form Nb_3Sn filaments. A schematic of the process is shown in Fig. 1.

Niobium powder was isostatically compacted in rubber tubes to pressures of from 25 ksi to 50 ksi. A minimum presure was required to give the compact adequate green strength. Porosity of the green compact was controlled by the compaction pressure (Fig. 2).

Green compacts were vacuum sintered at 2200°c to 2300°C for 5 min. to 40 min. at a pressure of 10^{-5} mm Hg, and then they were infiltrated with tin at 550°C to 750°C for 30 seconds. Both sintering and tin infiltration were carried out in an Abar furnace (Fig. 3).

On all but a few specimens, cladding was used to facilitate mechanical deformation and maintain integrity of the infiltrated rod. Monel, bronze (92% Cu, 8% Sn), or OFHC Cu was used as the cladding material. An intermediate sheath of tantalum prevented reaction between the cladding and the infiltrated tin. Tantalum or niobium could not be used as cladding material since they tend to gall on the dies.

The primary modes of deformation were wire drawing and hydrostatic extrusion. Form rolling was required on billets larger than 0.34 in. diameter since this was the largest size that could be wire drawn on the available equipment. Swaging was used to initially impart good mechanical bonding between the core and claddings and to point the wire for drawing. Hydrostatic extrusion was performed on a 250,000 psi 0.750 in. bore machine located at Stanford University, Department of Material Science. Figure 4 shows the hydorstatic extrusion machine from the rear along with the projectile barrier, the pumping station, and the protective screen around the control panel. Figure 5 is a side view of the machine with the water cooling system attached.

II. Analytcal Techniques

Optical microscopy was used to: 1) identify the various phases present; 2) evaluate the uniformity of tin in the niobium matrix, and 3) determine the volume fraction of tin present in the infiltrated compact. An anodization method developed by Picklesimer[13] gave a characteristic color to each phase: blue for Nb; yellow for Sn; reddish brown for Nb_6Sn_5; violet for Nb_3Sn. A typical photomicrograph of the as-infiltrated compact is shown in Fig. 6a. Although it was expected that only elemental niobium and tin should be present in the as-infiltrated compact, it was inportant to be able to distinguish the brittle Nb_6Sn_5 phase since its presence drastically lowers ductility and therefore has a deleterious effect on mechanical reduction of the rod. The volume fraction of tin was determined by a two-dimensional point count method.[14]

Scanning electron microscopy and EDAX (Energy Dispersive Analysis of X-rays) were used to determine fracture modes on the surface of tensile test specimens and to distinguish the phases present.

Tensile tests were made on as-infiltrated compacts to determine the effect of sintering time on ductility and porosity. Fifteen compacts were sintered, three at a time, at 2250°C for five periods of time varying from 5 min. to 40 min. The sintered rods were then infiltrated with tin at 600°C.

Compression tests were made on various cladding materials, niobium (both wrought and from powder) and Nb-Sn as-infiltrated compacts for estimating material flow stresses at hydrostatic extrusion strain rates.

RESULTS AND DISCUSSION

Conductor Length Requirements

One of the motivations for fabricating long lengths of superconducting wire is to be able to make a superconducting solenoid and to test it. To determine the lengths of superconducting wire which would be required, a solenoid was designed using the computer code "SOLEB" written by F. Voelker at the Lawrence Berkeley Laboratory (Appendix). The solenoid was envisioned to be wound with multicore wire having six superconducting cores and one center copper core for added stability. Each core was to be 0.015 in in diameter. The solenoid was designed for 100 kgauss with the wire carrying 600 amps. This value of current was derived from Hemachalam's work and includes a 10% margin of safety against quenching. A design curve for the minimum amount of wire needed for various solenoid geometries is given in Fig. 7.

Compact Processing

Initial attempts to directly scale up the powder metallurgy process for making Nb_3Sn superconducting wire using Hemachalam's parameters were unsuccessful. Consequently, the influence of powder size, compaction pressure, sintering time, and infiltration temperature was evaluated. Niobium powder of -270 mesh from Wah Chang was used. The green porosity as a function powder size fraction and compaction pressure is shown in Fig. 2. An isostatic compaction pressure of 30 ksi gave adequate porosity along with the required green strength. Sintering temperatures of 2250 to 2300 °C appeared to be satisfactory. Infiltration temperatures of 700°C and 750°C were found to cause the formation of Nb_6Sn_5 (Fig. 6b). Rods that had been infiltrated at these temperatures tended to fracture at the early stages of wire drawing. Rods infiltrated at lower temperatures did not always wet completely which resulted in areas that were void of tin (Fig. 8). To resolve this problem, the sintered rod was preheated to 600°C and infiltrated with tin at 600°C. The result was a completely infiltrated rod with no Nb_6Sn_5 present, provided that the tin bath was reasonably clean.

Besides core fracturing encountered during wire drawing, cladding fracture also occurred. Annealed monel was used as cladding for wire drawn rods since Hemachalam had the most success with it in his work. During form rolling, which was requried for the initial size reduction, the cladding was subjected to large alternating strains. This plastic cycling of the monel usually resulted in the eventual fracture of the cladding, either in the last stages of form rolling or during the pointing of the wire on the swaging machine. To circumvent the problem of sleeve fracture two rods, one

0.19 in. diameter and the other 0.45 in. diameter, were deformed without cladding. The exposed tin on the surface of the rods both prevented galling and acted as an excellent lubricant. The drawing force appeared to be much less for these unclad rods than for clad rods. The 0.19 in. diameter rod was reduced in area by a factor of 50 and still had tin remaining in it (Fig. 9). The 0.45 in. diameter rod was reduced in area by a factor of 800 and had no tin remaining (Fig. 10). The tin apparently squeezed out of the rod on the up stream side of the die. It was therefore deemed necessary to have cladding to prevent tin squeeze out during wire drawing at higher reductions.

Tensile tests were performed to see what effect sintering time had on the mechanical properties of the as-infiltrated rods and on the volume fraction of tin in the rods. The results are shown in Figs. 11, 12, and 13. As expected, ductility, as indicated by reduction in area and % elongation, increased with sintering time, and percent volume fraction of tin decreased with sintering time. It should be noted that the 25 min. and particularly the 40 min. test specimens had pores that were void of tin. This is to be expected since it is generally accepted that at porosities less than 10% most of the pores are isolated and therefore cannot be infiltrated. The unexpected decrease in strength with increasing sintering time is presumed to be a result of grain growth. The fracture surfaces of the tensile specimens were observed using an SEM and the fracture mode determined. The 5 min. and 10 min. specimens showed a fair amount of cleavage fracture (Fig. 14, and 15) whereas the other specimens showed no indication of cleavage fracture as exemplified by the 40 min. specimen which shows "internal necking"[15] (Fig. 16).

Hydrostatic Extrusion

Because of the difficulties encountered with wire drawing, hydrostatic extrusion was tried as an alternate method of mechanical reduction. Hydrostatic extrusion of Nb_3Sn wire and NbTi wire have been reported in references 16 and 17. Hydrostatic pressure has been shown to increase the ductility of various materials that are subjected to tension.[18] An application of this finding was to extrude materials under hydrostatic pressure; in addition to increasing the ductility of the material being extruded, hydrostatic extrusion eliminates the container wall friction associated with conventional extrusion and also provides for a certain amount of lubrication between the billet and the die.[19,20]

Hydrostatic extrusion was initially attempted on two 0.5 in. diameter as-infiltrated rods (No. 1 and 2, Table 1), and a 0.625 in. diameter sintered Nb rod (No. 3, Table 1). In these first extrusions billet design was somewhat arbitrary and both core instability and cladding fracture were encountered. Rather than proceeding blindly to determine under what conditions a successful extrusion could be made,

B. Avitzur[21,22] was consulted because he has done much work in the area of how process parameters affect both wire drawing and hydrostatic extrusion. He has also determined under what conditions successful coextrusions can be made.[17,23,24] Recently, Avitzur has developed a computer code based on theoretical analysis to determine acceptable core to sleeve diameter ratios and acceptable reductions to prevent core or sleeve fracture given the die angle, flow stress ratios, and billet-die friction coefficient.[25] To determine the flow stresses for the various materials that were extruded compression tests were made at different strain rates. Flow stress versus strain rate was plotted on a log-log graph (Fig. 17), since most metals follow the relationship $\sigma_f = \sigma_o \dot{\varepsilon}^m$ where σ_o and m are constants.[26] In this way, the flow stress at strain rates encountered during extrusion can be extrapolated. Based on information given by the code, a fourth billet was designed and extruded (No. 4, Table 1). A comparison between Nos. 3 and 4 is made in Fig. 18. The results seem to correspond well to Avitzur's predictions since the process parameters of No. 3 were within the core instability or fracture region given by his computer code and No. 4 was not.

Since billet No. 4 extruded successfully, five more billets (Nos. 5 through 9) were either made or modified to conform to Avitzur's criteria. Figures 19 and 20 are photographs of billets Nos. 5 and 8 before their first extrusion pass. Figure 21 is a photograph of billet No. 8 after its first pass, and Fig. 22 shows it made into a billet for a second reduction. The billets had mild steel plugs at the ends so that the extrusion would stall out prior to reaching the end of the billet. Billet No. 6 virtually exploded out of the machine in many pieces (Fig. 23), and billet No. 9 did not extrude at a 94% reduction in area, and the machine broke down when a reduction of 88% was tried. Billets Nos. 5, 7 and 8 extruded with uniform cores on the first reduction and no sleeve fractures except for billet No. 5 pass 3 (Figs. 24, 25 and 27). During this extrusion, the Nb-Sn core appeared to have pulled the monel in tension and fractured it. This was attributed to the relatively high cladding to core flow stress ratio and therefore monel is not recommended for use as cladding material. The second extrusion of billet No. 8 resulted in a fractured product (Fig. 26). Photomicrographs of the Nb-Sn cores of billets Nos. 5 and 8 after a 69% and 77% reduction, respectively, reveals a fairly uniform dispersion of Sn filaments (Figs. 27 and 28). At a total reduction in area of 95% for billet No. 8 fissures appeared towards the centerline of the core and oriented themselves approximately 45° to the core axis (Fig. 29). Also, it was observed that tin tends to flow into these fissures. A similar observation was made for billet No. 7 (Fig. 30). It seems plausible that this tin segregation may have resulted from pressure differentials between interconnected pores due to the low flow stress of tin particularly in the liquid state (all the extrusions of Nb-Sn showed evidence of tin melting despite water cooling of the extrusion product during deformation). Lending support to this explanation for the tin segregating: Rogers, et al.,[27] has determined stress solutions for sheet drawing by slip-line analysis which reveals a hydrostatic compression component near the dies but a hydrostatic tensile component at the centerline of the sheet. Although Rogers' data cannot be directly related to axisymmetric extrusion, Lambert and Kobayashi[28] have demonstrated similar trends for axisymmetric extrusion. An as-infiltrated rod wire drawn to a total reduction in area of 91% exhibits the same segregation of tin to the center of the rod (Figs. 31 and 32).

CONCLUSIONS

1. Increasing the diameter of infiltrated compacts to produce long lengths of multifilamentary Nb_3Sn wire as suggested by Hemachalam proved to be more difficult than expected. Re-evaluation and refinement of the process parameters has been made but more work in this area is required.

2. The optimum temperature for tin infiltration now appears to be 600°C provided that the sintered rod is preheated to 600°C prior to infiltration. This procedure will ensure proper wetting of the niobium rod resulting in complete infiltration and will prevent the formation of the brittle Nb_6Sn_5 phase.

3. To maintain a uniform and sufficient proposity in the 1/2 to 3/4 in. diameter nobium rod, sintering times ranging from 15 to 20 min. appear to be optimal for a sintering temperature of 2250°C. Further refinement in this area should be pursued, particularly in reference to powder particle size distribution.

4. Form rolling prior to wire drawing usually results in cladding failure. A larger and more sophisticated draw bench would eliminate the need for form rolling.

5. Reduction in areas of up to 80% could be achieved by hydrostatic extrusion without apparent damage to the infiltrated core.

6. It appears desirable to maintain the ratio of the cladding flow stress to core flow stress close to or less than 1.

ACKNOWLEDGEMENT

The author wishes to thank Prof. M. R. Pickus for his guidance. Additional thanks to Dr. J. L-F. Wang for his comments and suggestions, and to Dr. K. Hemachalam for his help in the early stages of this work. The technical advice of J. T. Holthuis was of great value. The assistance of J. A. Jacobsen with metallorgraphic techniques was greatly appreciated.

Special thanks are due to Professor O. Sherby of Stanford Univeristy for his interest in this project, and for not only making available the use of thie hydrostatic extrusion machine, but also for setting up a cooperative effort with their research technician, Rob Whalen, whose contributions were invaluable. Thanks also to Professor B. Avitzur of Lehigh University for his recommendations regarding optimization of the extrusion parameters. I greatly appreciate the fruitful discussions with Professors F. E. Hauser and S. Kobayashi of the University of California at Berkeley.

This work has been accomplished under the auspices of the U. S. Energy Research and Development Administration through the Materials and Molecular Research Division of the Lawrence Berkeley Laboratory

APPENDIX

```
L

      *%SOLEB% SOLENOID LOAD LINE
      1Ø     READ,LMAX,DS,H,D,W,XI,TH
             NMAX=25
             T=D+TH
             DØ=DS
             D1=DS+D
             BE=H/DØ
             N1=AINT(H/W)
             LT=PI*D1*N1/12
             PRINT, N1, DØ, BE, T
             NLP=1
             DO 5Ø I=1,NMAX
             NLP=NLP+1
             D2=DS+2*T*NLP-D
             D3=D2+D
             N=NLP*N1
             AL=D3/DØ
             X=1.2567/2.54/DØ/(AL-1)
             X1-AL+SQRT(AL*AL+BE*BE)
             X2=1+SQRT(1+BE*BE)
             X3=X*ALOG(X1/X2)
             HF=N*XI*X3
             L=PI*D2*N1/12
             LT-LT+L
      PRINT8, N, HF, D3, AL, LT
             IF(LT.GE.LMAX) GO TO 1Ø
      5Ø     CONTINUE
             GO TO 1Ø
 OK - ^EDIT
```

REFERENCES

1. H. K. Onnes, Comm. Phys. Lab., University of Leyden, 119, 120, 122 (1911).

2. J. E. Kunzler, E. Buehler, F. S. L. Hsu and J. H. Wernick, Phys. Rev. Letters, 6, 89 (1961).

3. M. G. Benz, IEEE Trans. on Magnetics, Vol. Mag-2 No. 4, 760 (1966).

4. K. Tachikawa and S. Fukuda, Trans. Nat. Research Inst. Metals, 9, 39 (1967).

5. M. Suenaga and W. B. Sampson, Appl. Phys. Letters, 18, 584 (1971).

6. M. Suenaga and W. B. Sampson, Appl. Phys. Letters, 20, 443 (1972).

7. M. N. Wilson, C. R. Walters, J. D. Lewin and P. F. Smith, J. Physics D, 3, 1517 (1970).

8. M. R. Pickus and J. L-F. Wang, Paper presented at the International P/M Conf. 1976, LBL 5121, May 1976.

9. B. N. P. Babu, M. S. Thesis, LBL-437, December 1971.

10. T. N. Garrett, M. S. Thesis, LBL-448, December 1971

11. K. Hemachalam, M. S. Thesis, LBL-1108, June 1972.

12. K. Hemachalam, D. Eng. Thesis, LBL-4181, February 1976.

13. M. L. Picklesimer, U.S.A.E.C., Oak Ridge National Laboratory, Report 2296 (1957).

14. E. E. Underwood, Metals Handbook, Vol. 8, ASM, 1973.

15. J. F. Knott, Fundamentals of Fracture Mechanics, John Wiley, 1973.

16. Battelle Columbus Lab., Prog. Rep. "Experimental Evaluation of Hydrostatic Extrusion for the Fabrication of Multifilament Superconducting Wire", May 23, 1975.

17. J. M. Story, B. Avitzur and W. C. Hahn, Jr., J. of Eng. for Ind., 98, (3), August 1976.

18. P. W. Bridgman, J. Appl. Phys. 18, 246, 1947.

19. B. I. Beresnev, L. F. Vereschagin, Y. N. Ryabinin and L. D. Livshits, Some Problems of Large Plastic Deformation of Metals at High Pressures, Pergamon Press, 1963.

20. H. Ll. D. Pugh and A. H. Low, J. of the Inst. of Met., 93, 1964-1965.

21. B. Avitzur and W. M. Evans, Wire J., 2, 11, November 1969.

22. B. Avitzur, Wire J., 7, 11, November 1974.

23. Boaz Avitzur and B. Avitzur, J. of Eng. for Ind., 92, 2, May 1970.

24. W. C. Hahn, Jr., and B. Avitzur, Prog. Rep. "Forming of Composite for Superconducting Rod", Inst. for Met. Form., Lehigh University, February 1972.

25. This work has not been published and therefore the design curves are not shown.

26. J. F. Alder and K. A. Phillips, J. Inst. Metals, 83, 80, 1954.

27. H. C. Rogers, R. C. Leech and L. F. Coffin, Jr., Bur. of Nav. Weap. Final Rep., Cont. No. 63-0671-c, July 1964.

28. E. R. Lambert and S. Kobayaski, Proc. Ninth Int'l MTDR Conf. Univ. of Manchester, September 16-20, 1968.

TABLE I

Billet No.	Core and Diameter (in.)	Cladding and Diameter (in.)	Pass No.	Die Angle	Diameter Ratio Core/ Cladding	Flow Stress Ratio Cladding/ Core	Reduction in Area	Extrusion Pressure (psi)	Final Diameter (in.)	Remarks	Figure Nos.
1	Nb-Sn 0.450	Brass 0.735	1	45°	0.6	0.90	75%	* N/A	0.375	Sleeve fracture.	
2	Nb-Sn 0.450	None	1	45°	---	---	N/A	---	---	Billet buckled.	
3	Nb 0.625	Cu 0.735	1	45°	0.85	0.70	75%	N/A	0.367	Good extrusion.	
	0.312	0.735	2	45°	0.42	0.70	75%	N/A	0.375	Core fractured.	18
4	Nb 0.250	Bronze 0.360	1	22°	0.69	1.38	73%	152,000	0.187	Good extrusion, uniform core.	18
5**	Nb-Sn 0.450	Monel 0.640	1	22°	0.70	1.35	80%	250,000	---	Did not extrude.	
	0.450	0.640	2	22°	0.70	1.35	69%	160,000	0.355	Uniform core, rough surface.	19, 24, and 27.
	0.450	0.600	3	22°	0.75	1.35	65%	160,000	0.357	Nb-Sn forced out cladding fracturing it in tension.	
6	Nb-Sn 0.723	None	1	22°	---	---	75%	152,000	0.360	Fractured into many pieces.	23
7	Nb-Sn 0.40	Nb 0.535	1	22°	0.75	0.74	88%	N/A	0.187	Uniform core, rough surface.	25, 30, and 32.
	0.140	0.187	2	22°	0.75	0.74	55%	N/A	0.125	Uniform core, smooth surface.	
8**	Nb-Sn 0.400	OFHC Cu 0.555	1	22°	0.72	0.52	77%	160,000	0.266	Uniform core, smooth surface.	
	0.190	0.266	2	22°	0.72	0.52	78%	N/A	0.125	Both core and cladding fractured.	20, 21, 22, 26, 28, and 29.
	0.190	0.266	3	22°	0.72	0.52	78%	N/A	0.125	Both core and cladding fractured.	
9	Nb-Sn 0.400	OFHC Cu 0.556	1	22°	0.72	0.52	94%	250,000	0.125	Did not extrude.	
	0.400	0.556	2	22°	0.72	0.52	88%	---	---	Seals ruptured on machine.	

* N/A - Not available.

** Intermediate sheath of Tantalum tube 0.02 in. thick was put between core and cladding.

TABLE I -19-

FIGURE CAPTIONS

1. Schematic diagram of the filamentary wire fabrication process.
2. Green porosity vs. isostatic compaction pressure for different powders.
3. Schematic diagram of Abar furnace: (1) extension tube; (2) tantalum rod; (3) back filling port; (4) electrical leads; (5) heating element; (6) niobium specimen; (7) radiation shields; (8) water cooled wall; (9) W-5% Re vs. W-26% Re thermocouple junction; (10) vacuum connection; (11) quartz tube; (12) graphite crucible; (13) liquid Al-Ge eutectic alloy, and (14) resistance heater.
4. Hydrostatic extrusion machine from the rear with associated equipment.
5. Side view of hydrostatic extrusion machine with cooling system attached.
6. (a) an as-infiltrated compact: -270 mesh Nb powder, 30 ksi compaction pressure, 2250°C 15 min. sintering tempertature and time, and 600°C tin infiltration with Nb rod preheated to 600°C. (b) as-infiltrated compact with Nb_6Sn_5 formation (infiltration temperature 750°C).
7. Wire length requirements for various solenoid configurations.
8. Partially infiltrated wire. Darker areas indicate presence of tin.
9. Unclad reduced wire.

10. Unclad reduced wire.

11. Percent elongation and reduction in area vs. sintering time.

12. Percent volume fraction of tin vs. sintering time.

13. Yield strength and ultimate strength vs. sintering time.

14. Fracture surface of tensile specimen with EDAX display sintered for 5 min.

15. Fracture surface of tensile specimen with EDAX display sintered for 10 min.

16. Fracture surface of tensile specimen with EDAX display sintered for 40 min.

17. Log-log graph of flow stress vs. strain rate.

18. Comparison of billet designed to Avitzur's criterion; bottom, to that not designed to his criterion.

19. Billet No. 5.

20. Billet No. 8.

21. Extrusion of billet No. 8.

22. Billet made form extrusion of billet No. 8.

23. Extrusion of billet No. 6.

24. Extrusion of billet No. 5.

25. Extrusion of billet No. 7.

26. Second extrusion of billet No. 8.

27. Longitudinal section of billet No. 5 after 69% reduction.

28. Longitudinal section of billet No. 8 after 77% reduction.

29. Longitudinal section of billet No. 8 after a total reduction of 95%.

30. Longitudinal section of billet No. 7 after a total reduction of 95%.

31. Cross section of an as-infiltrated rod wire drawn to a total reduction of 91%.

32. Cross section of billet No. 7 extruded to a total reduction of 95%.

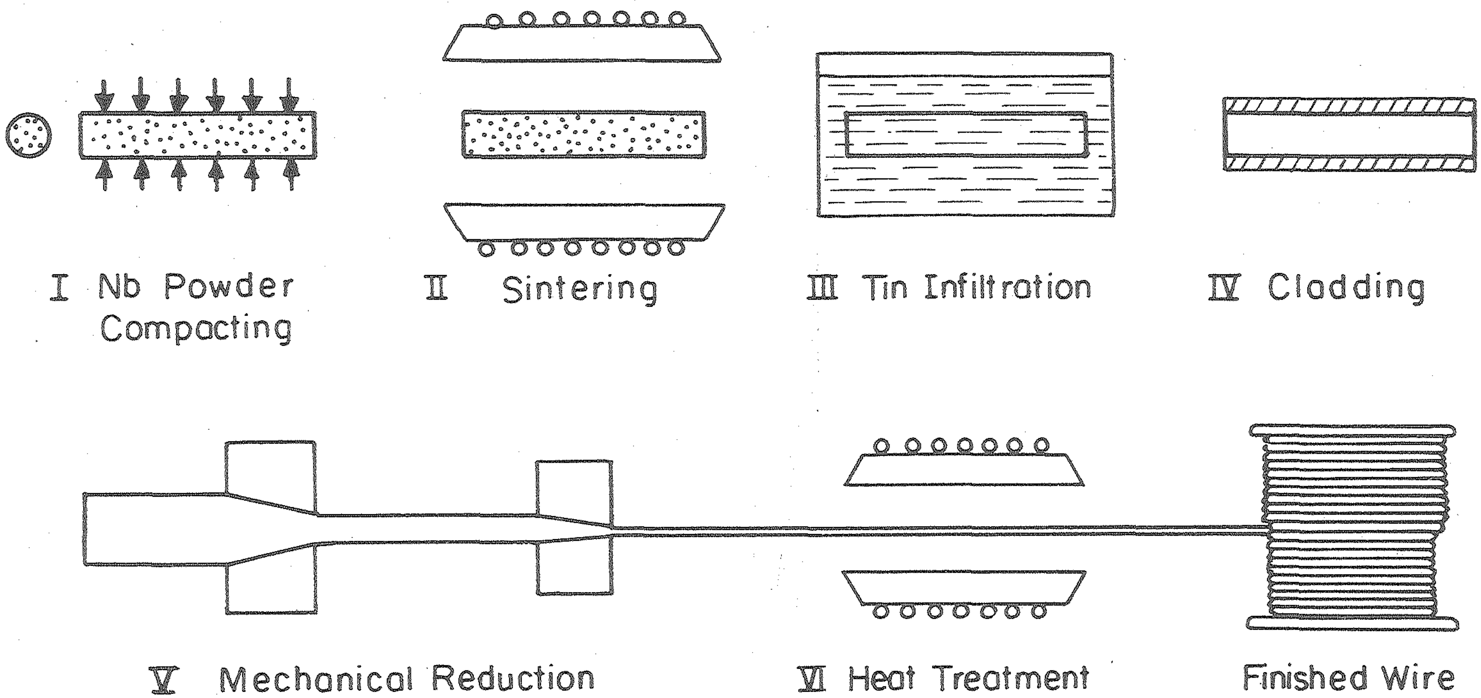

XBL 7510-7537

Fig. 1

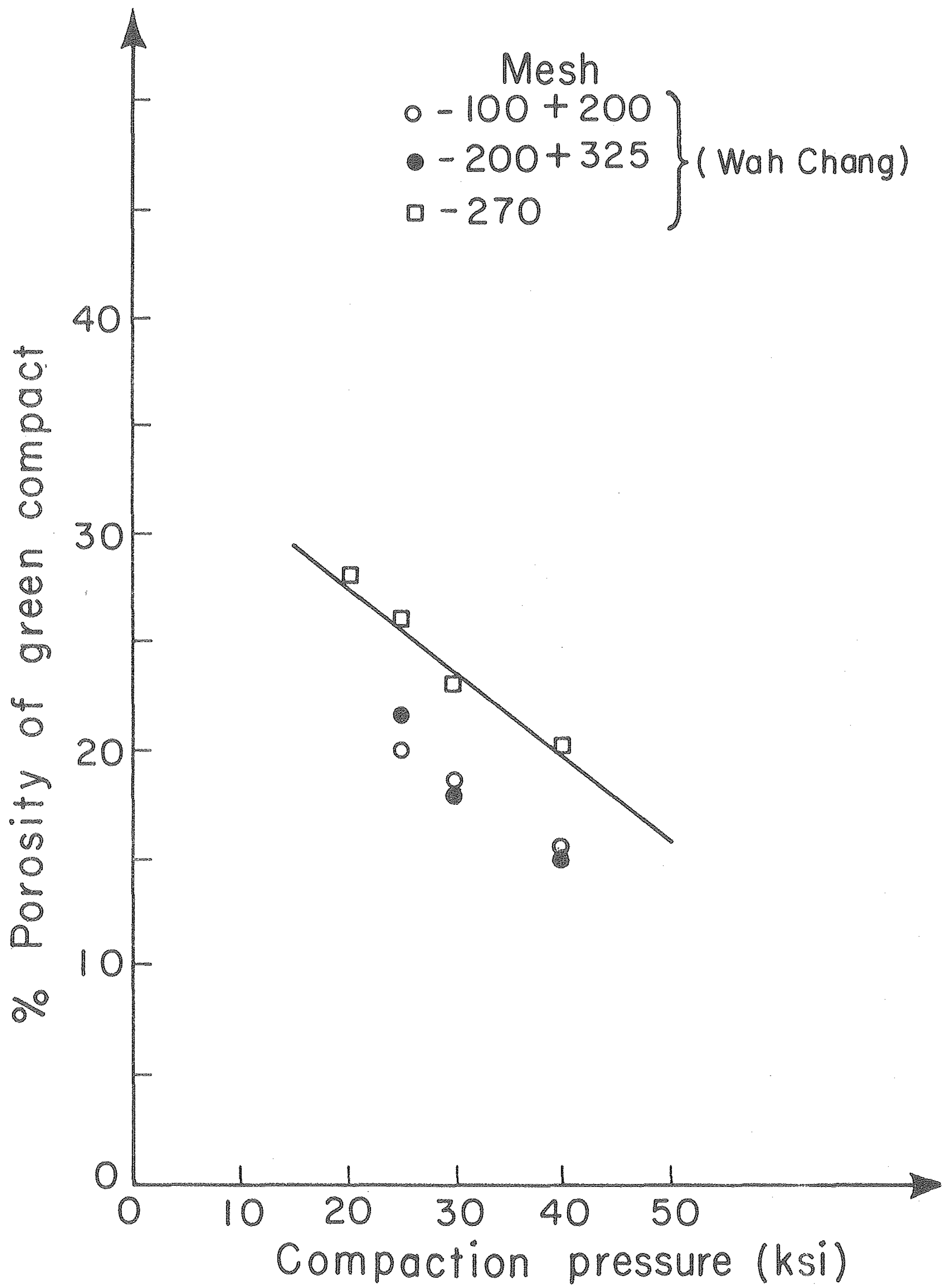

XBL776-1318

Fig. 2

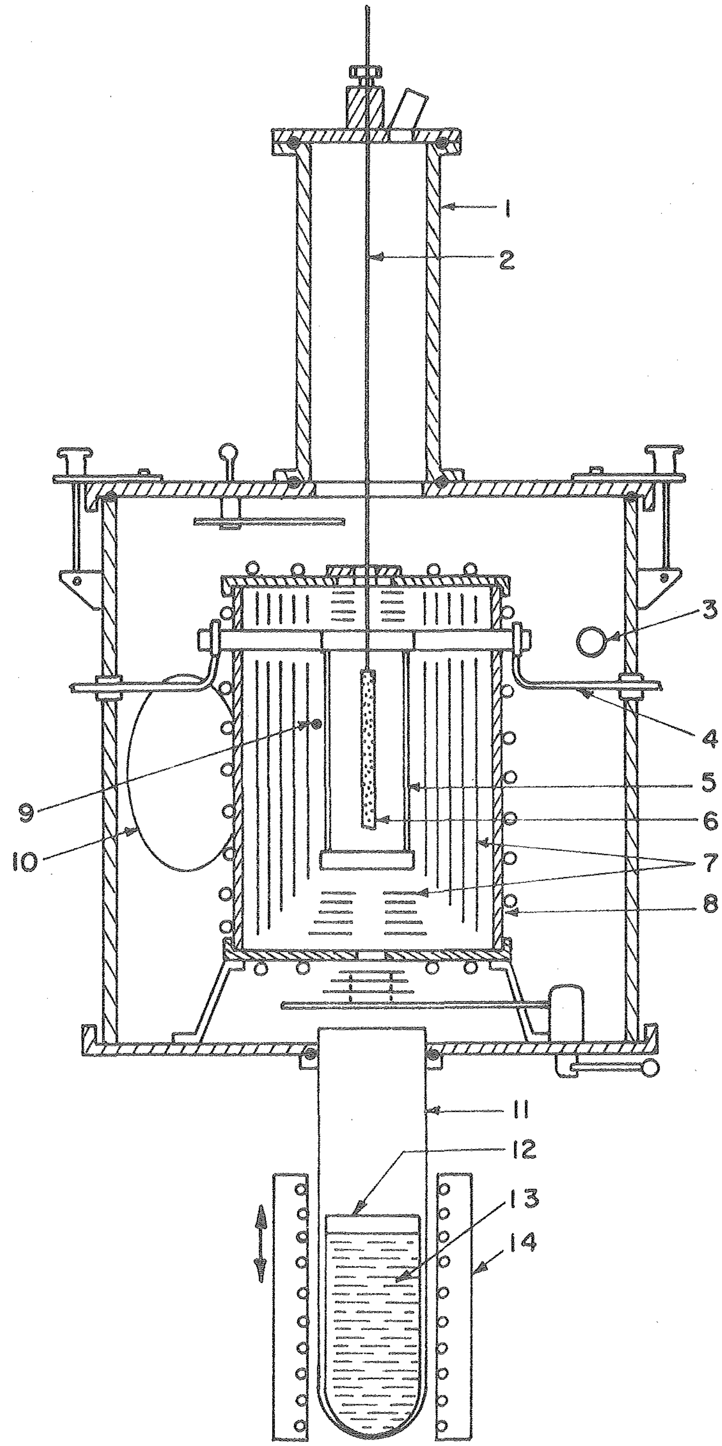

XBL 7210-7043

Fig. 3

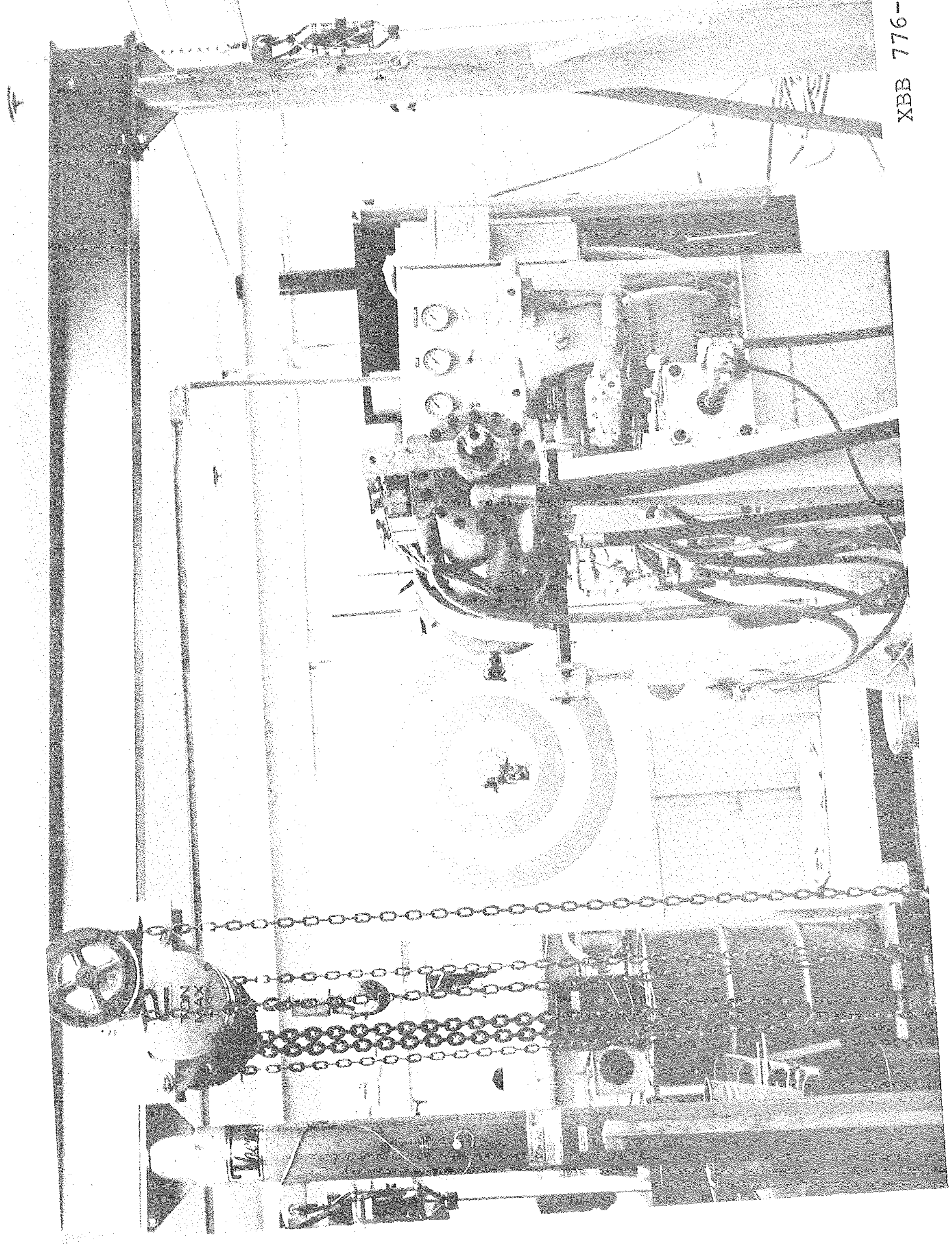

XBB 776-6083

Fig. 4

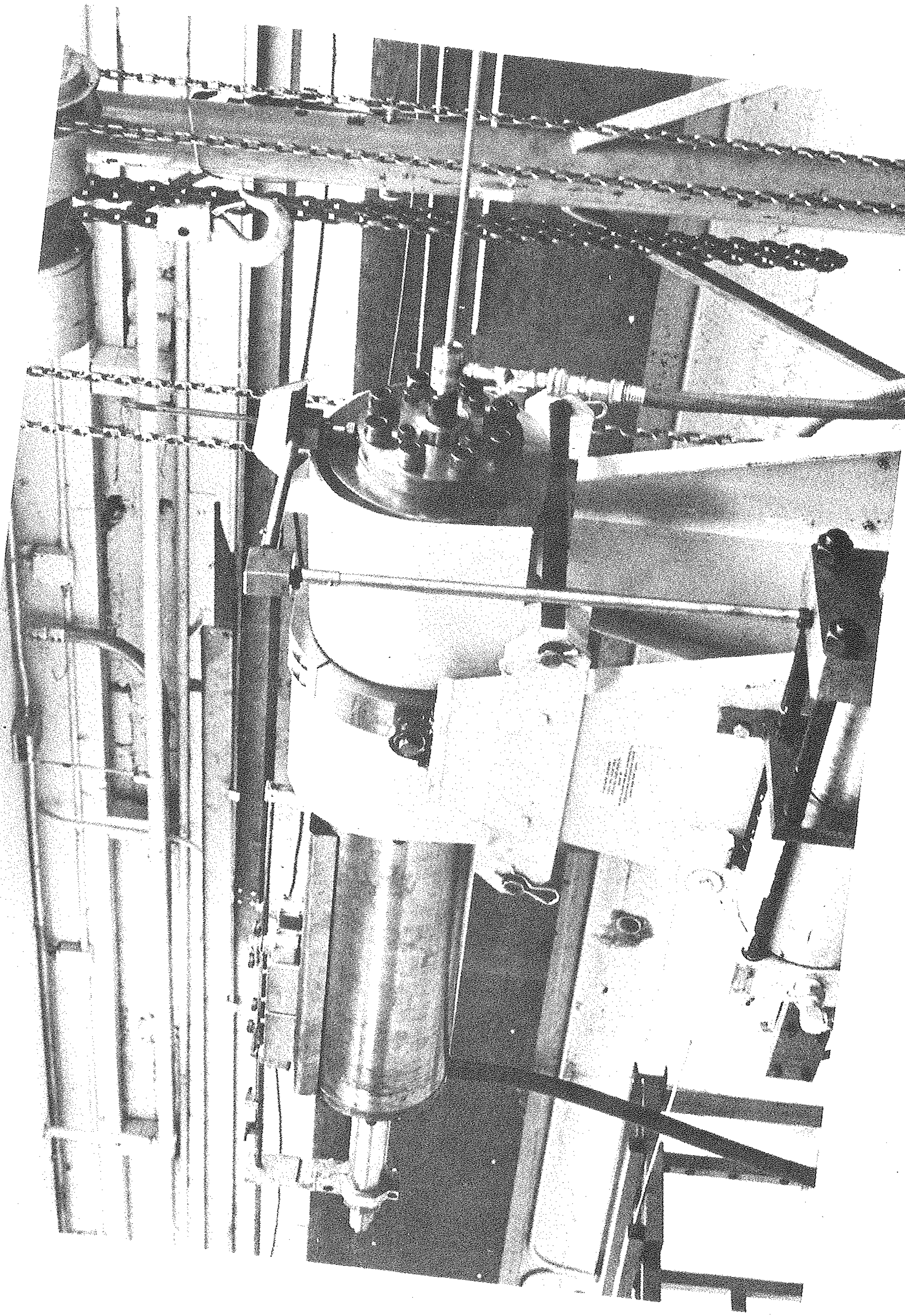

XBB 776-6085

Fig. 5

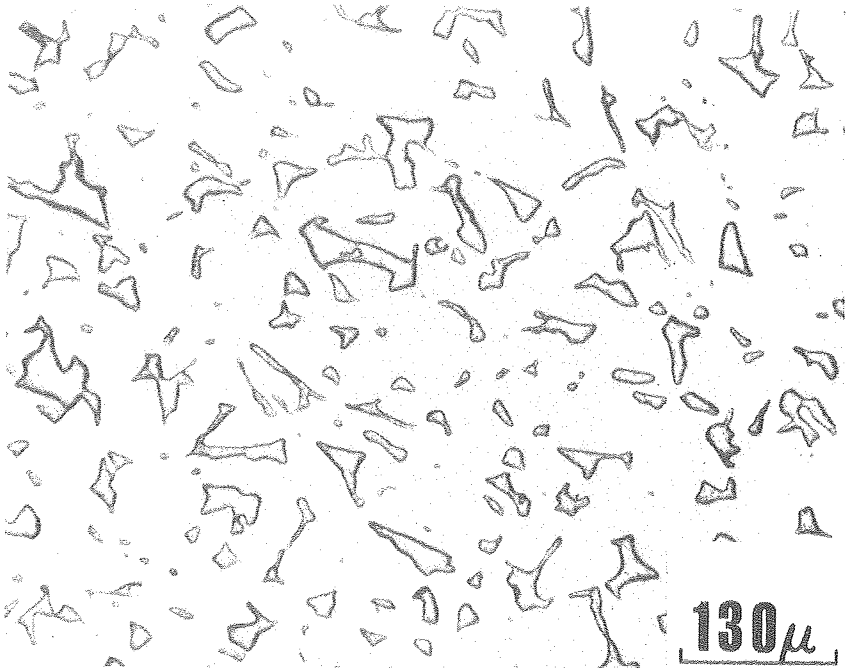

Fig. 6a

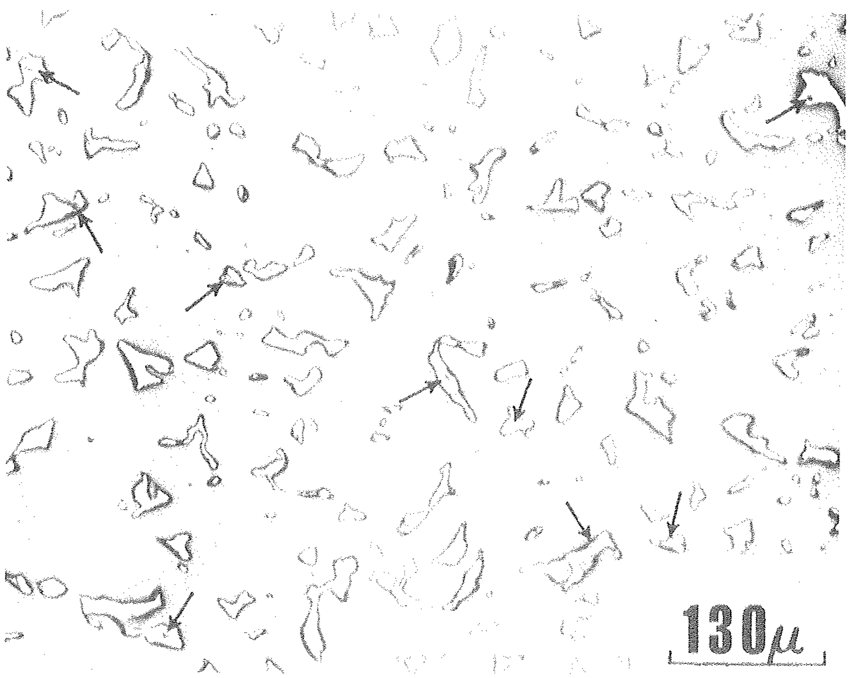

XBB 777-6291

Fig. 6b

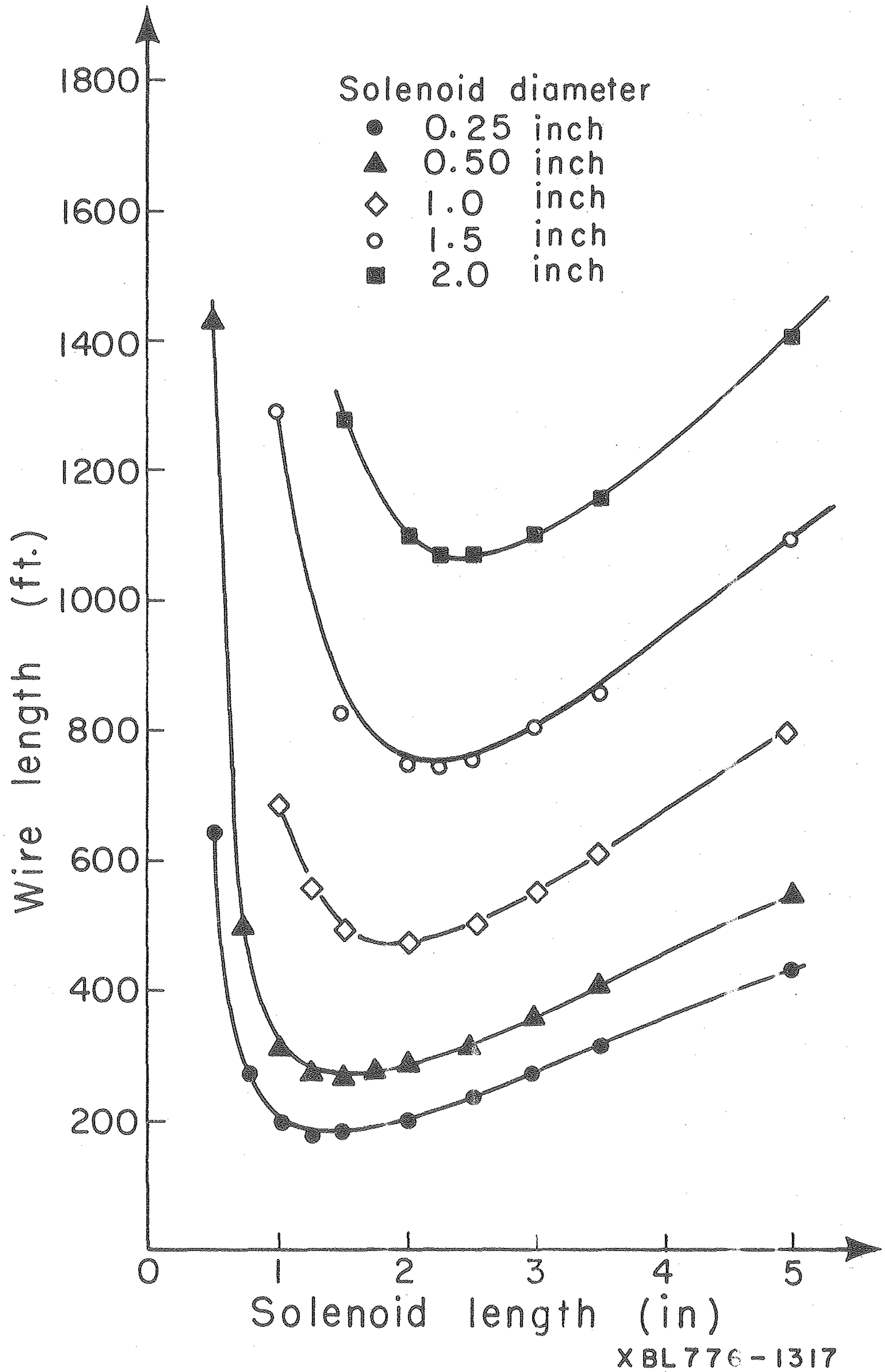

1800
1600
1400
1200
1000
800
600
400
200
Wire length (ft.)
Solenoid diameter
0.25 inch
0.50 inch
1.0 inch
1.5 inch
2.0 inch
0
1
2
3
4
5
Solenoid length (in)
XBL776-1317

Fig. 7

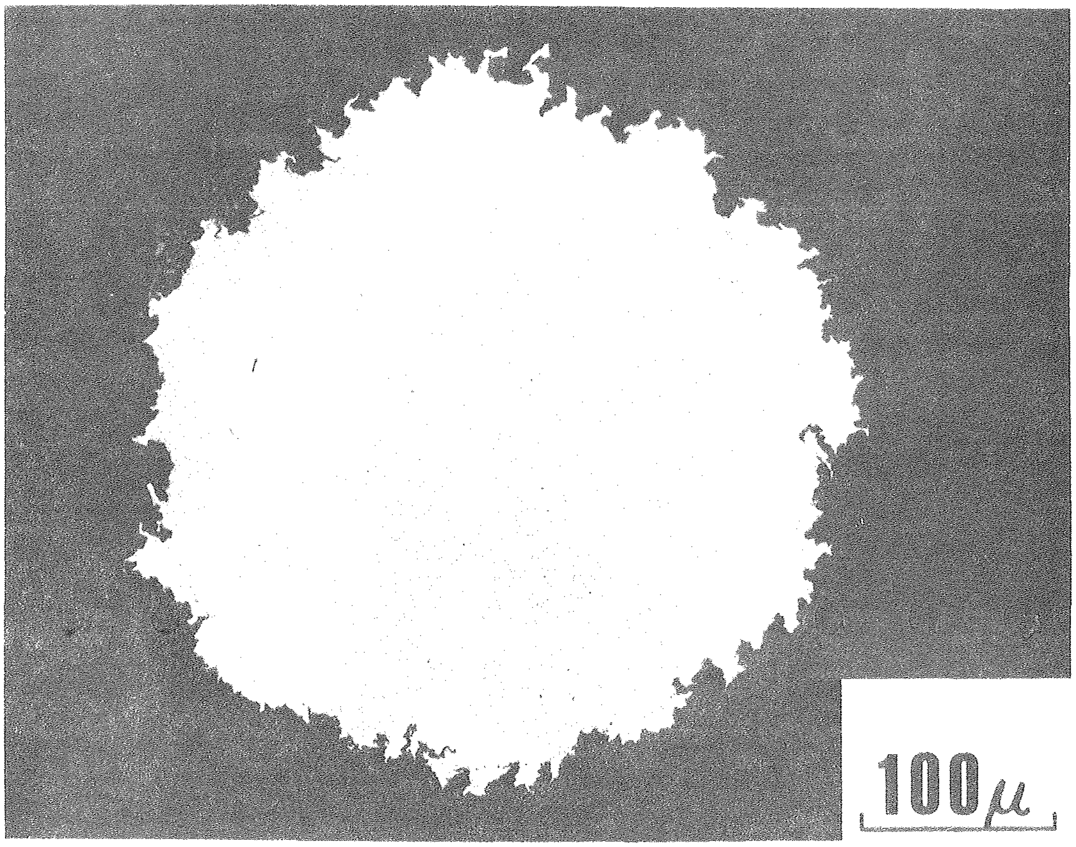

XBB 777-6298

Fig. 8

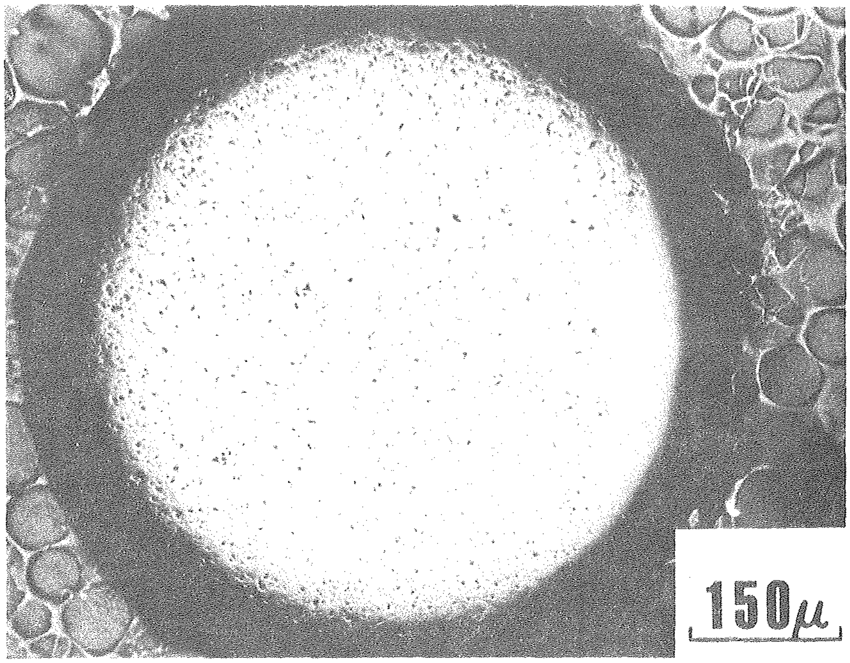

Fig. 9

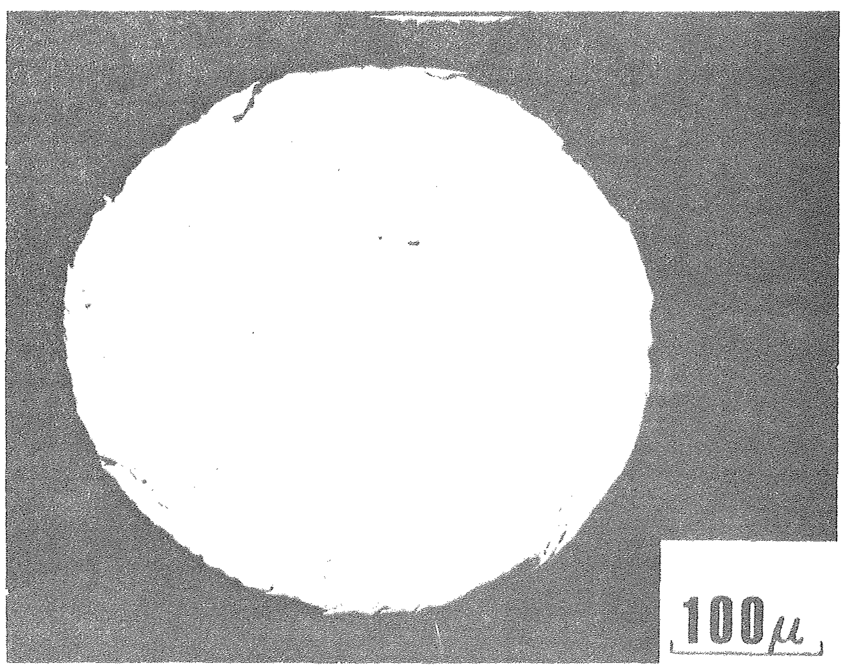

XBB 777-6298

Fig. 10

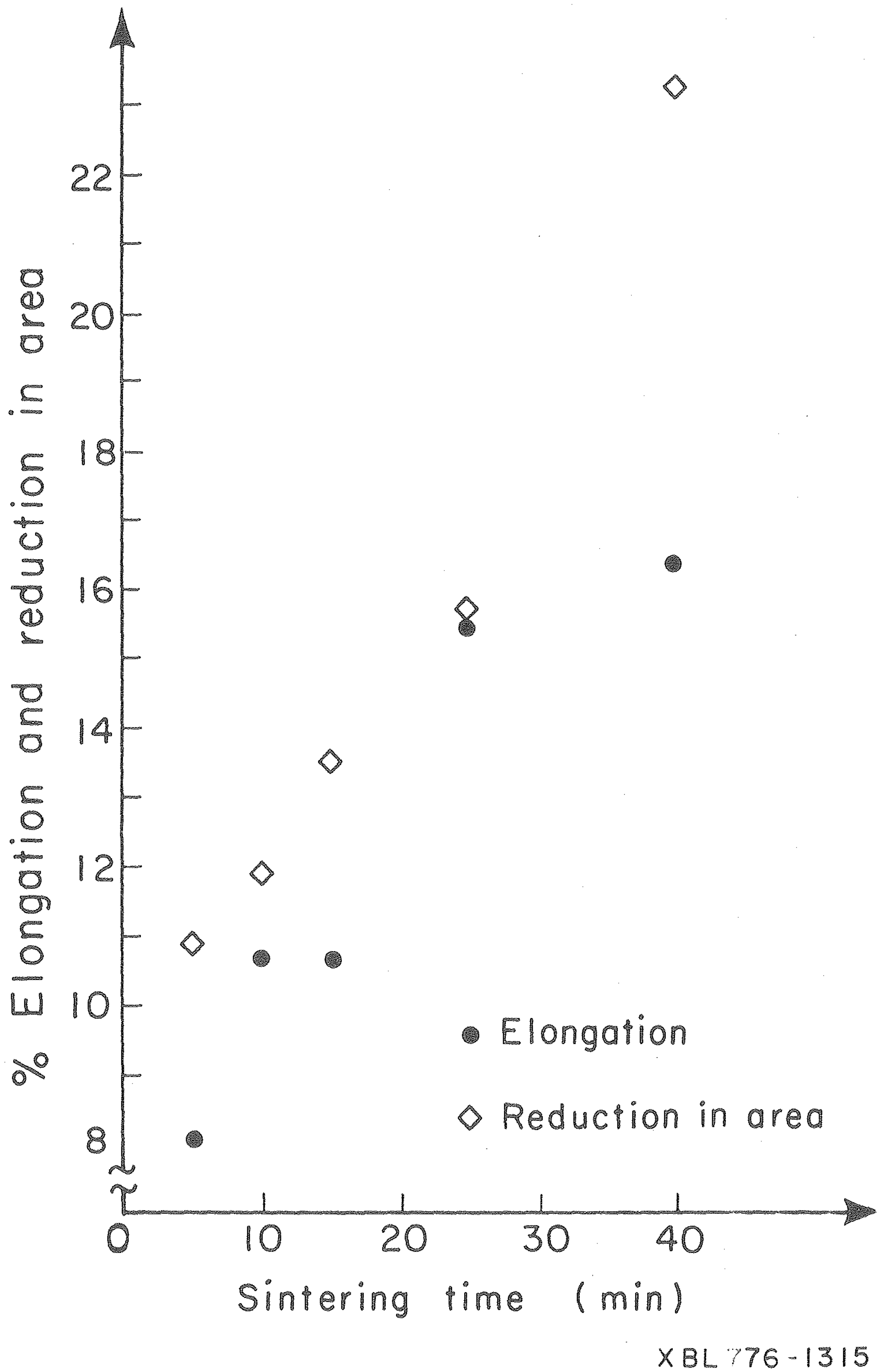
% Elongation and reduction in area
22
20
18
16
14
12
10
8
0
10
20
30
40
Sintering time (min)
Elongation
Reduction in area
XBL 776-1315

Fig. 11

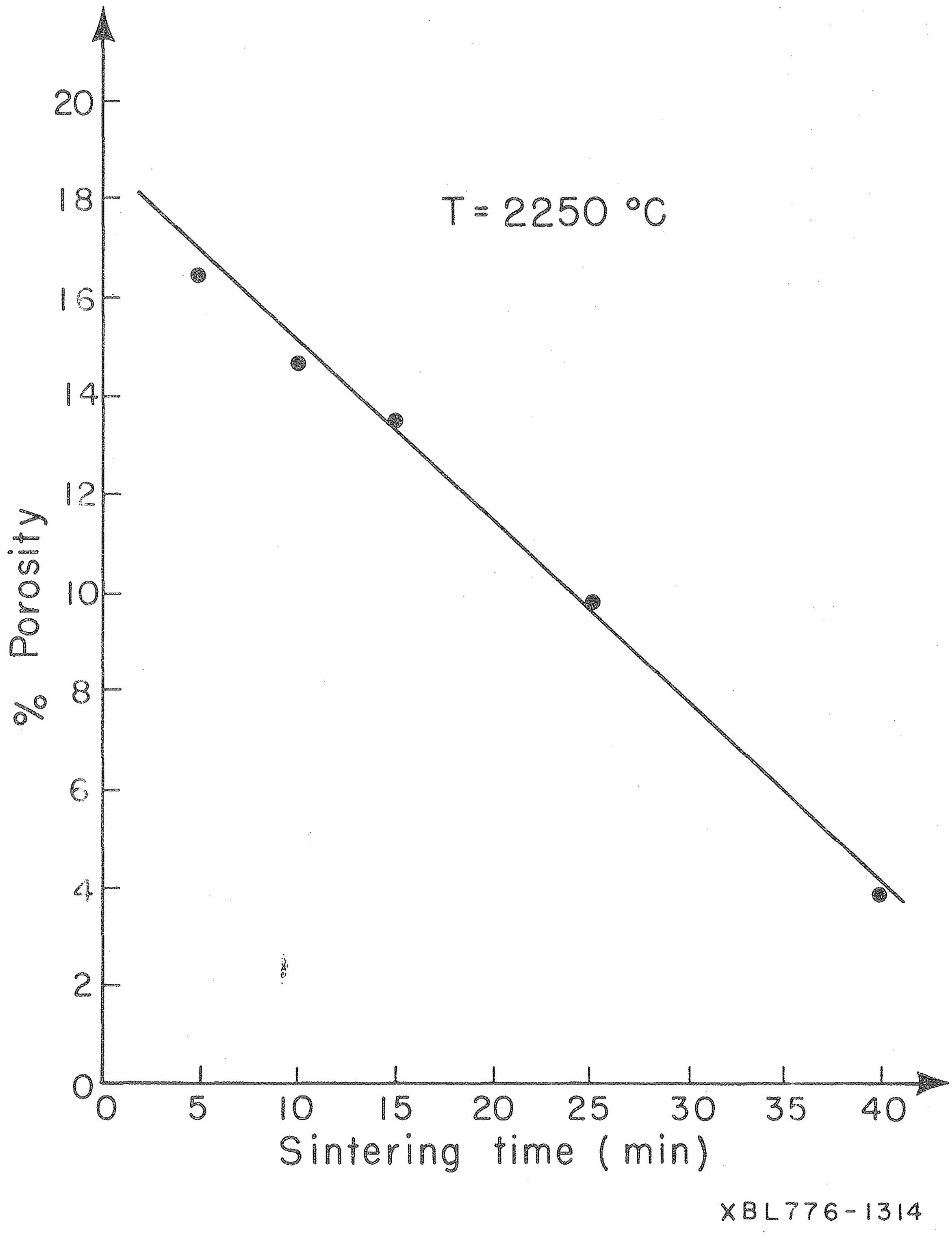
T= 2250 °C
20
18
16
14
12
10
8
6
4
2
0
% Porosity
0
5
10
15
20
25
30
35
40
Sintering time (min)
XBL776-1314

Fig. 12

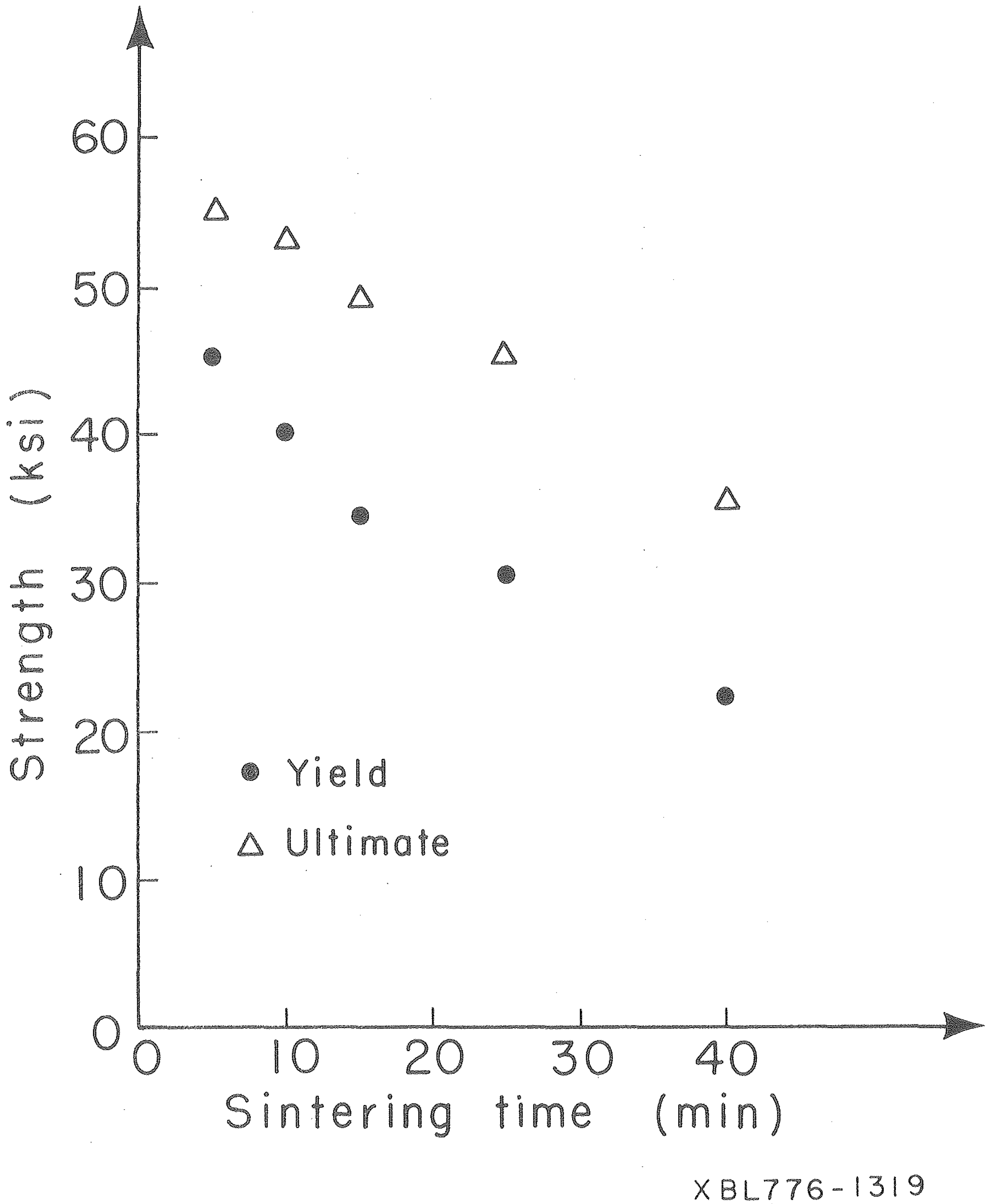

60
50
40
30
20
10
0
Strength (ksi)
Yield
Ultimate
0
10
20
30
40
Sintering time (min)
XBL776-1319

Fig. 13

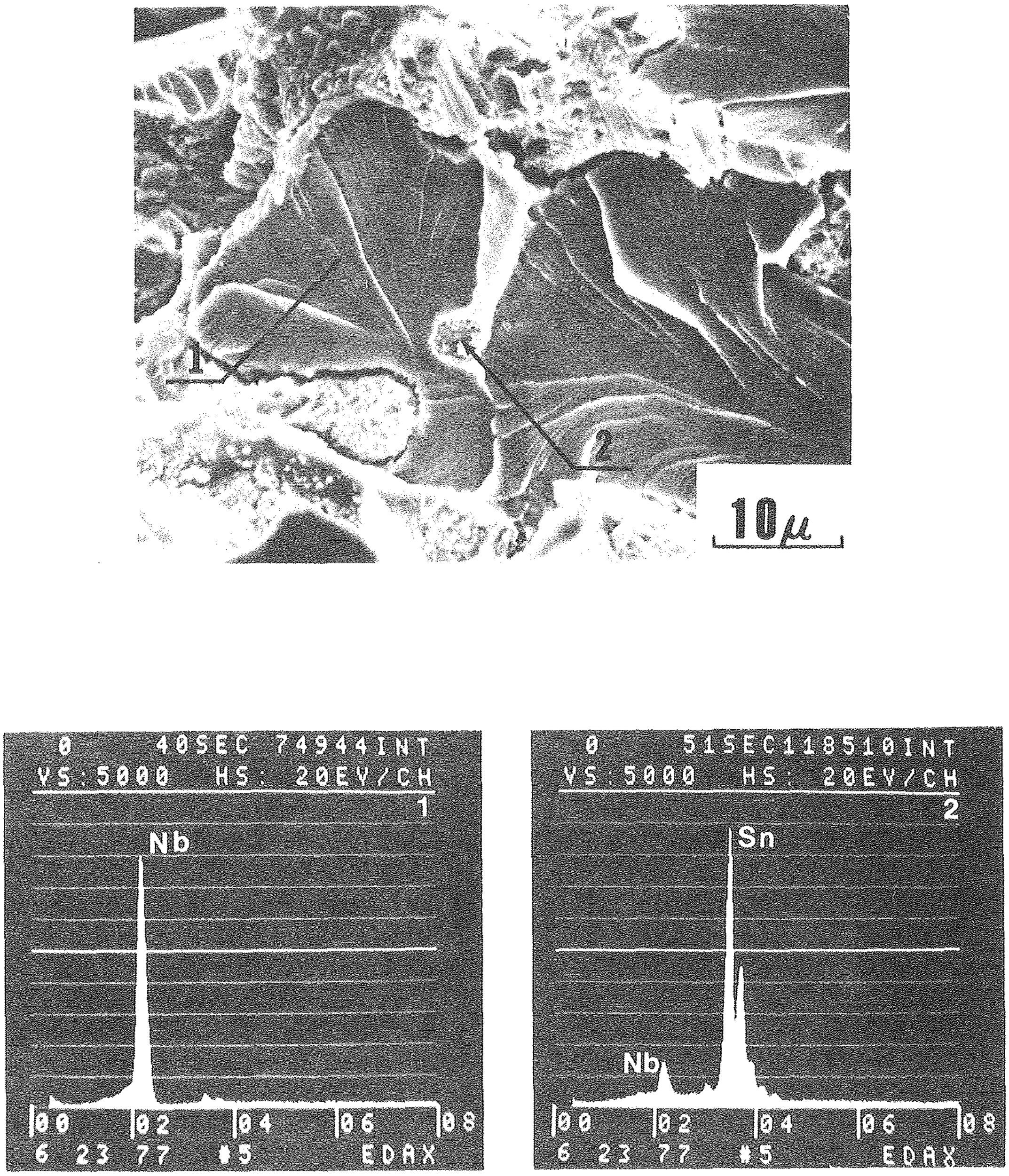

XBB 777-6293

Fig. 14

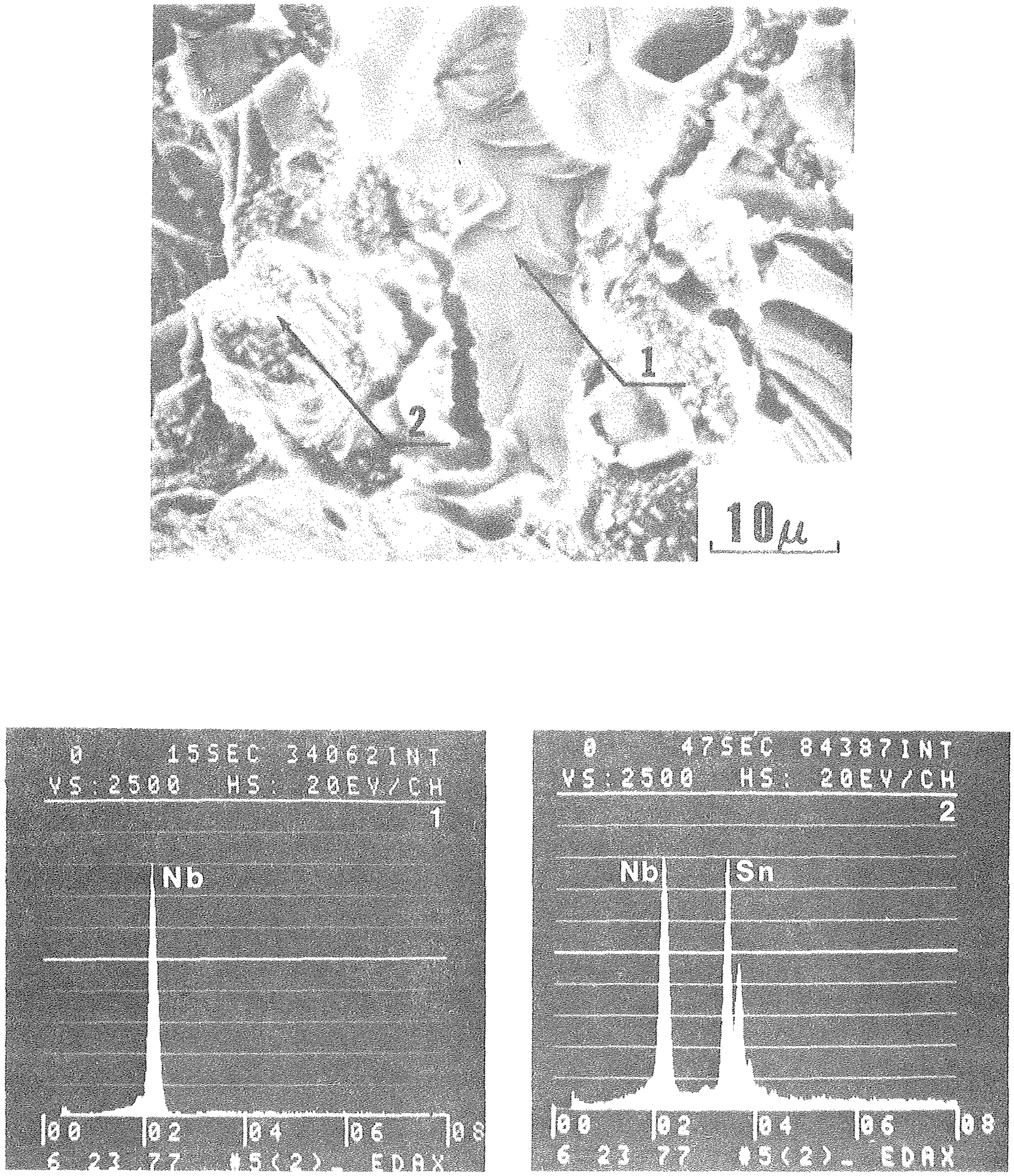

XBB 777-6294

Fig. 15

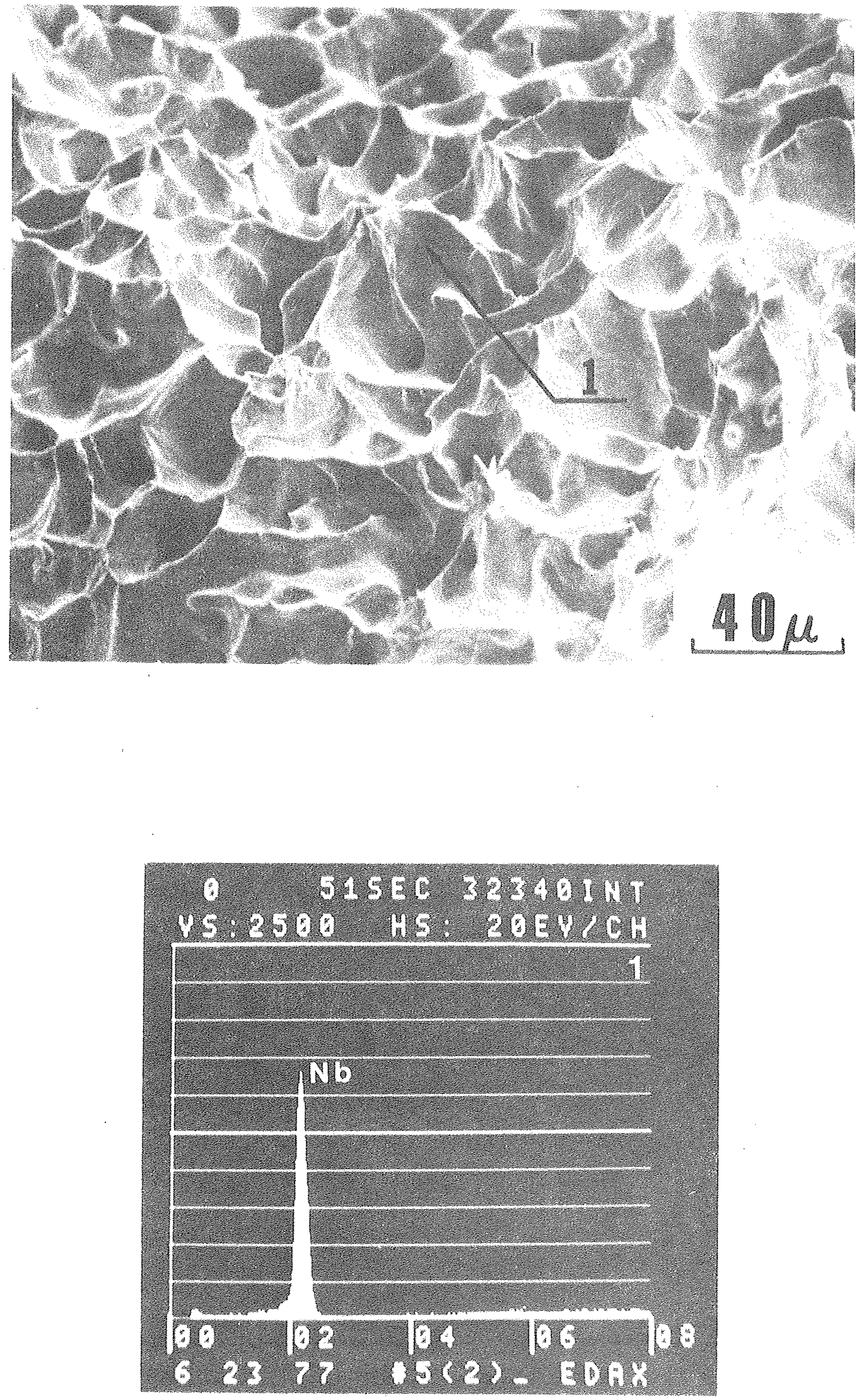

XBB 777-6295

Fig. 16

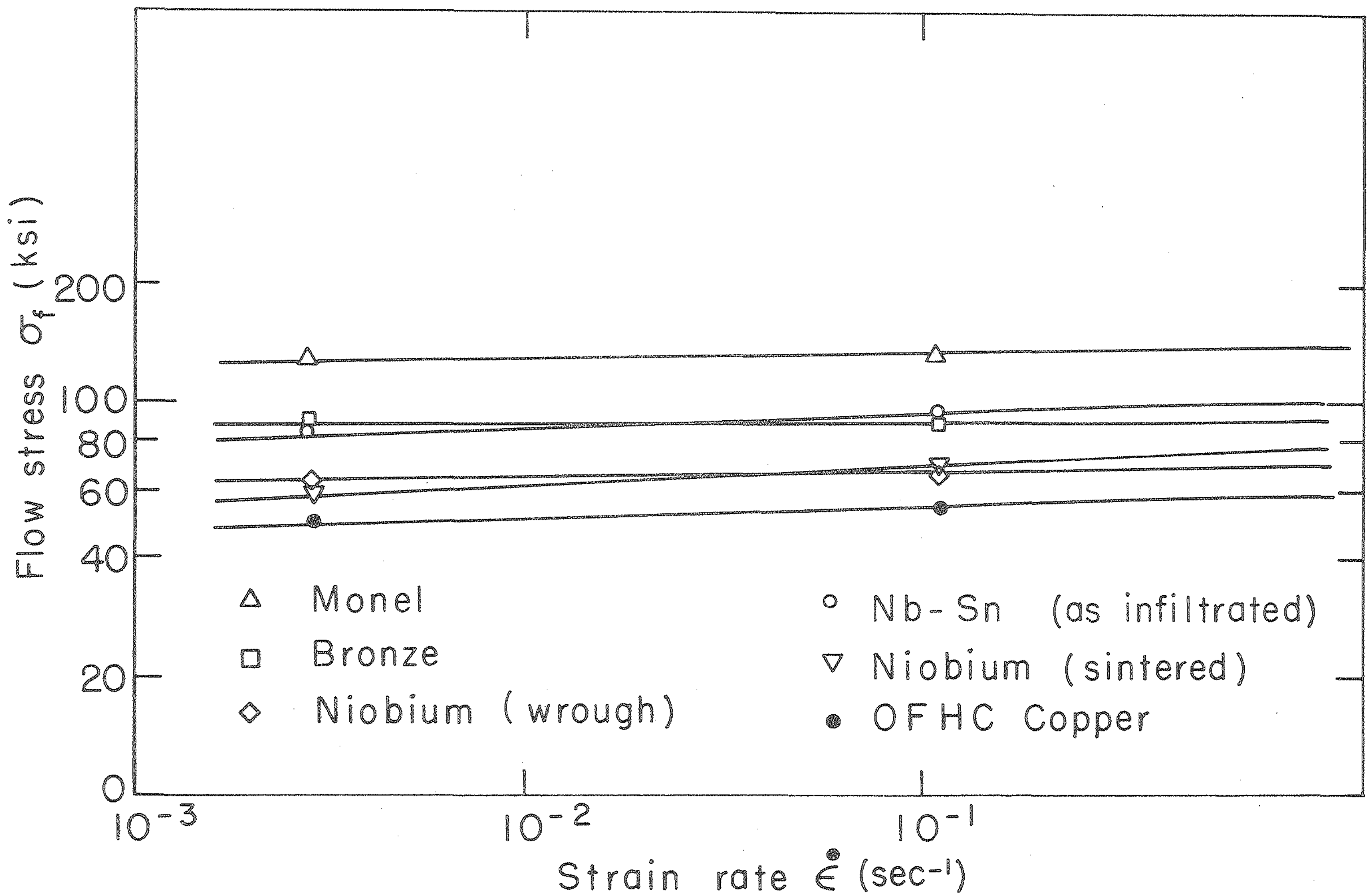

XBL776-1316

Fig. 17

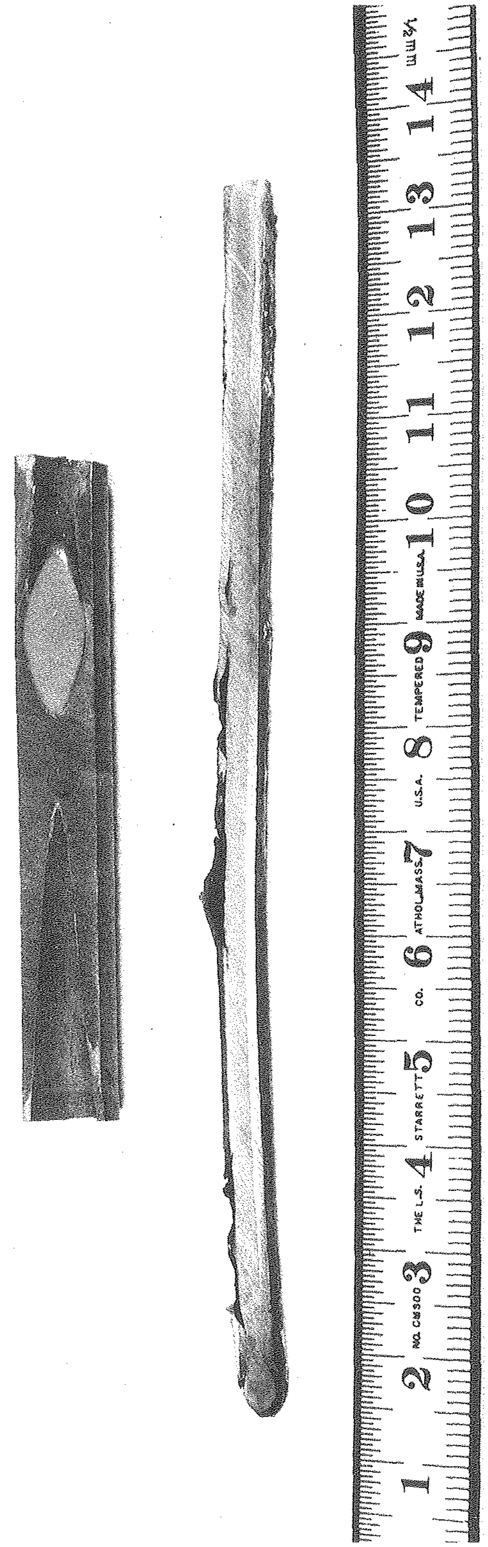

XBB 776-5910

Fig. 18

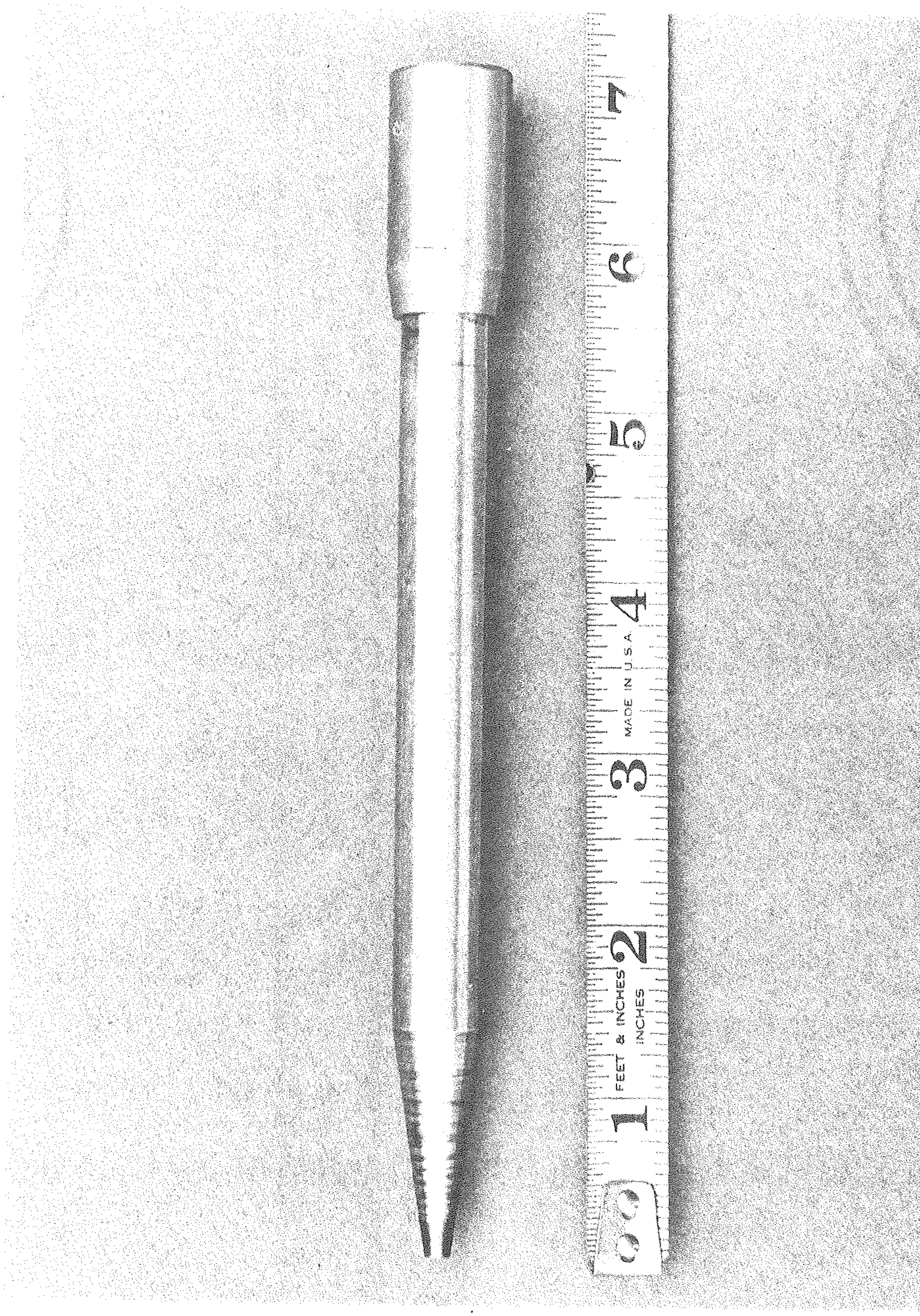

XBB 776-6086

Fig. 19

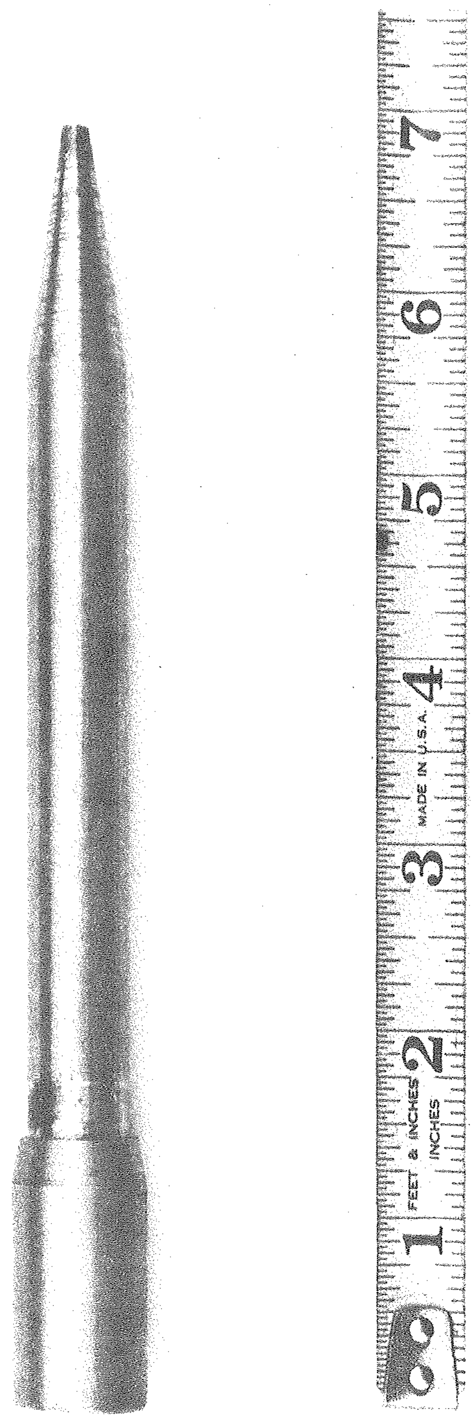

XBB 776-6087

Fig. 20

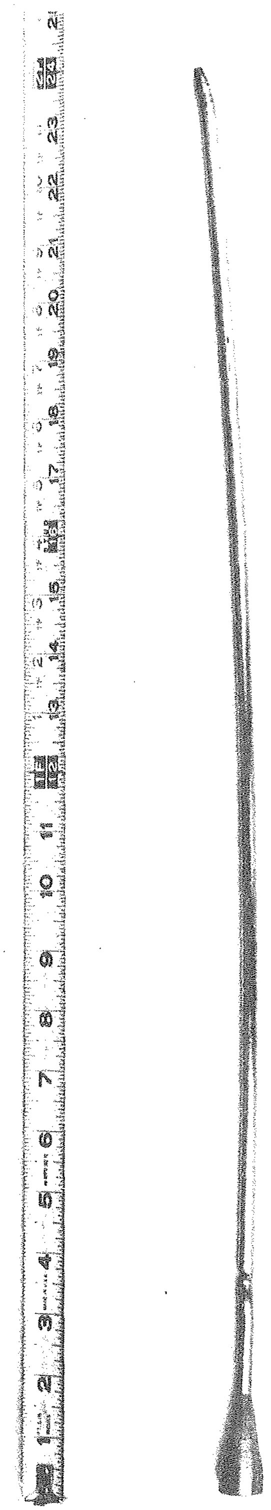

XBB 776-6084

Fig. 21

XBB 776-6082

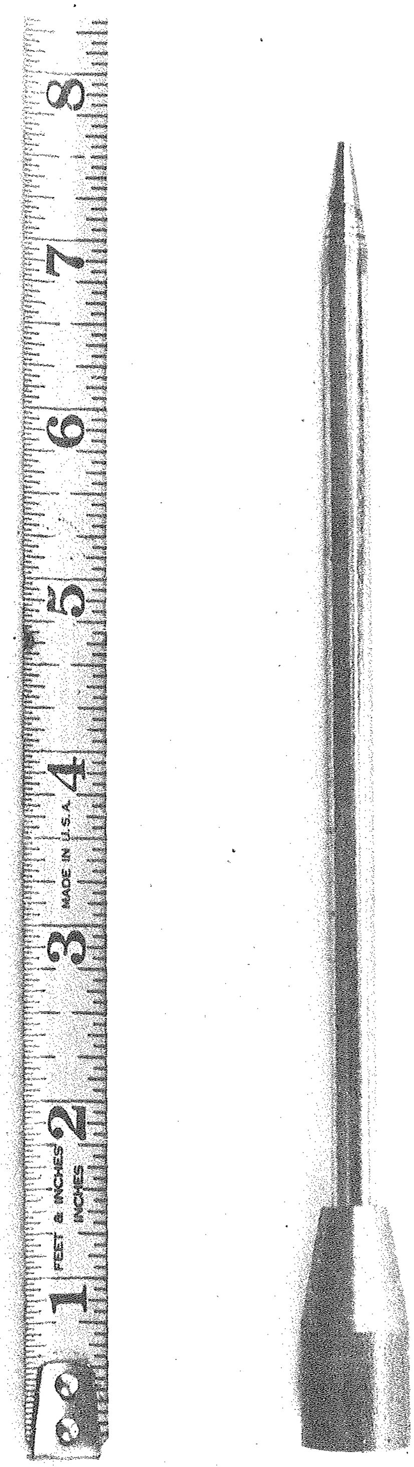

Fig. 22

XBB 776-5904

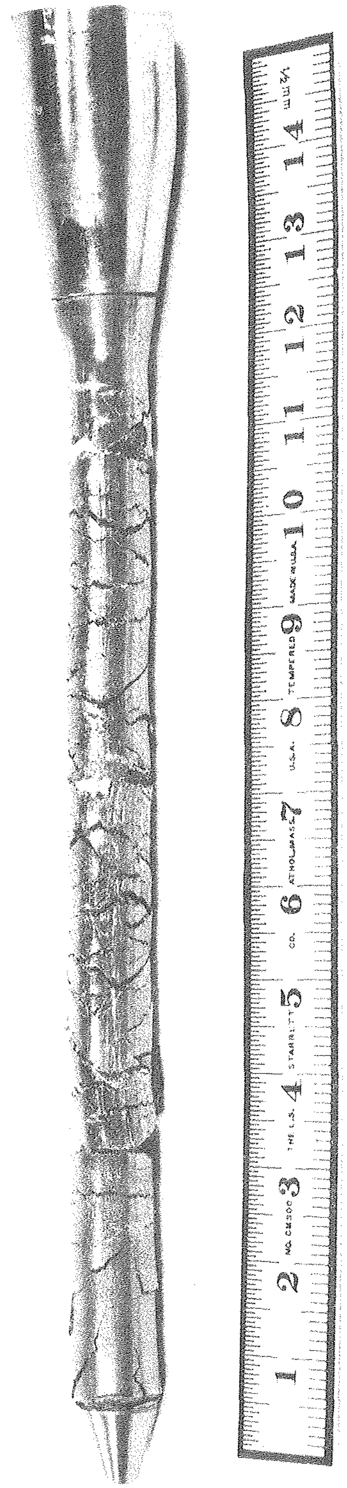

Fig. 23

XBB 776-5907

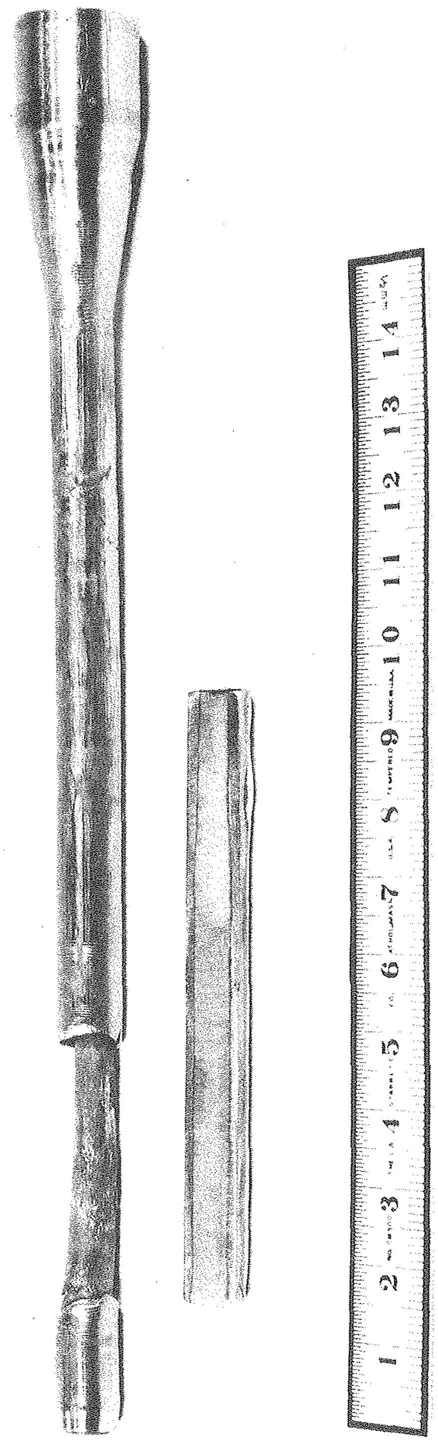

Fig. 24

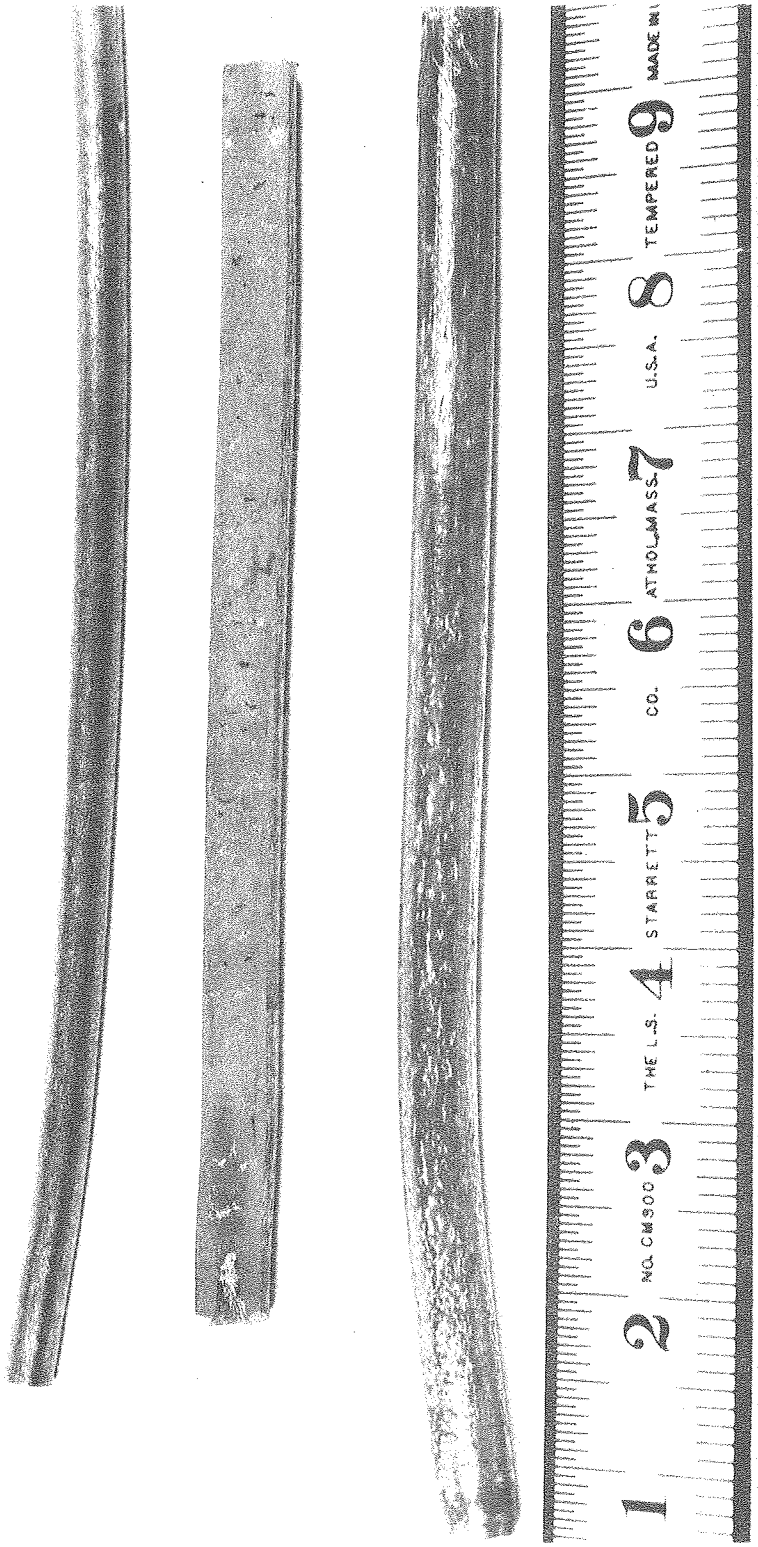

XBB 776-5903

Fig. 25

XBB 776-5905

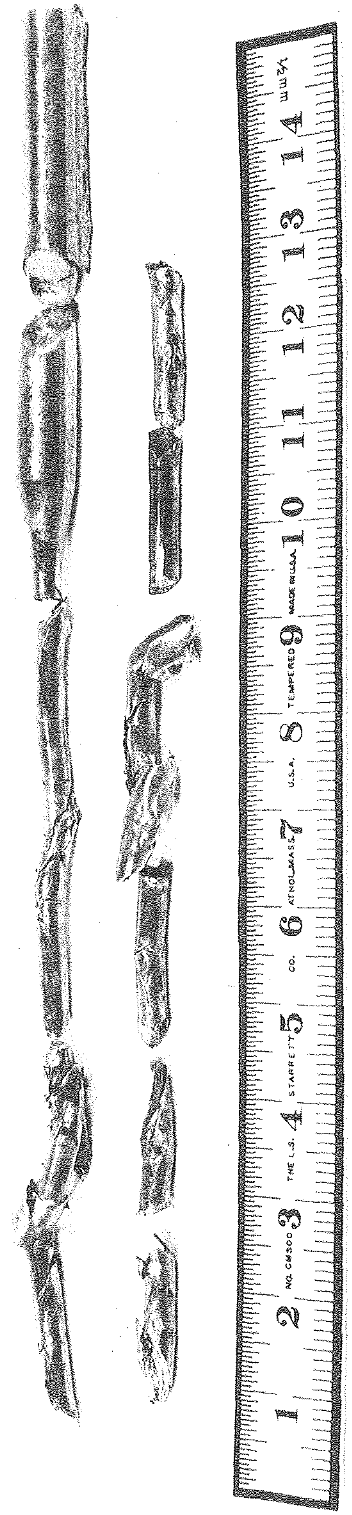

Fig. 26

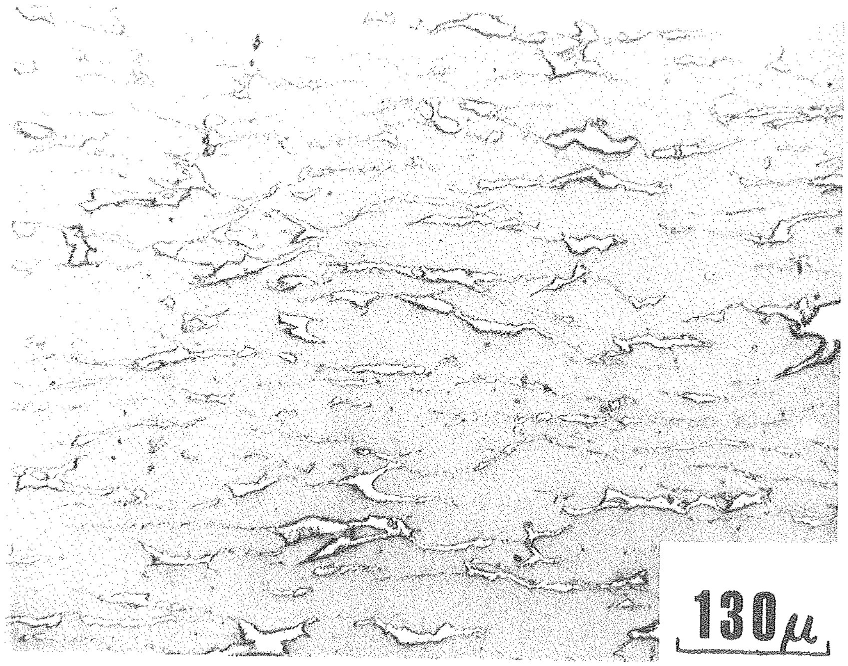

Fig. 27

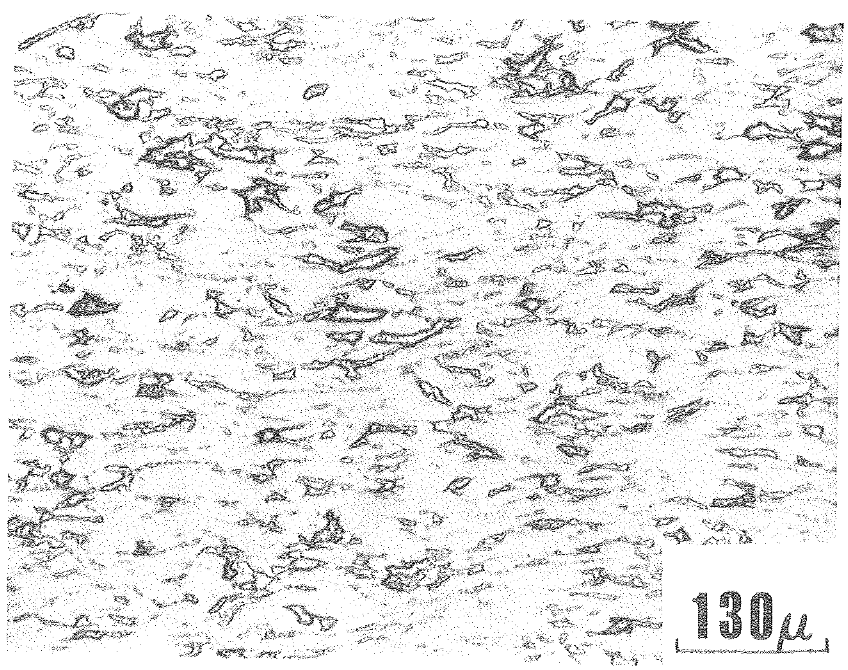

XBB 777-6296

Fig. 28

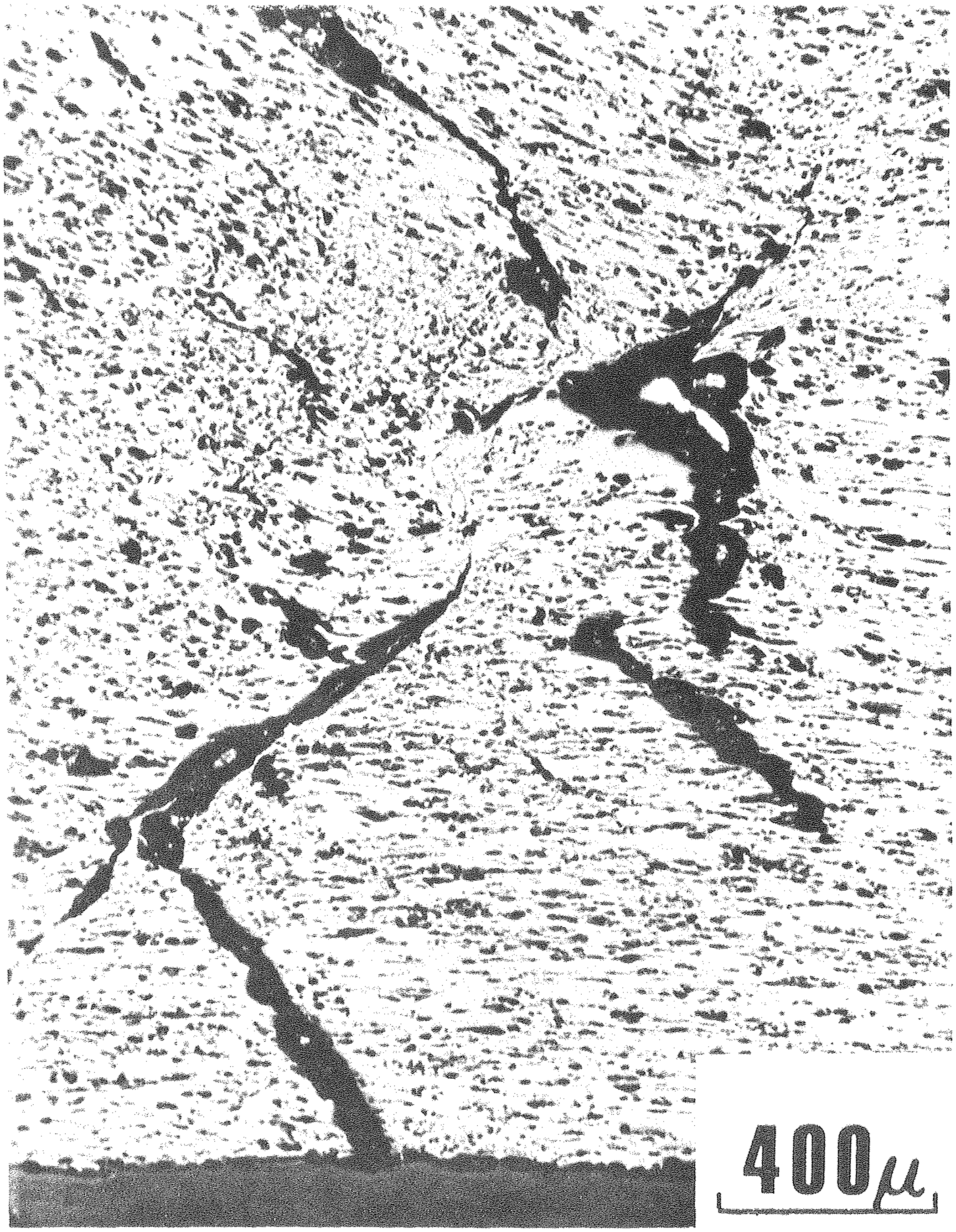

XBB 777-6297

Fig. 29

XBB 777-6297

Fig. 30

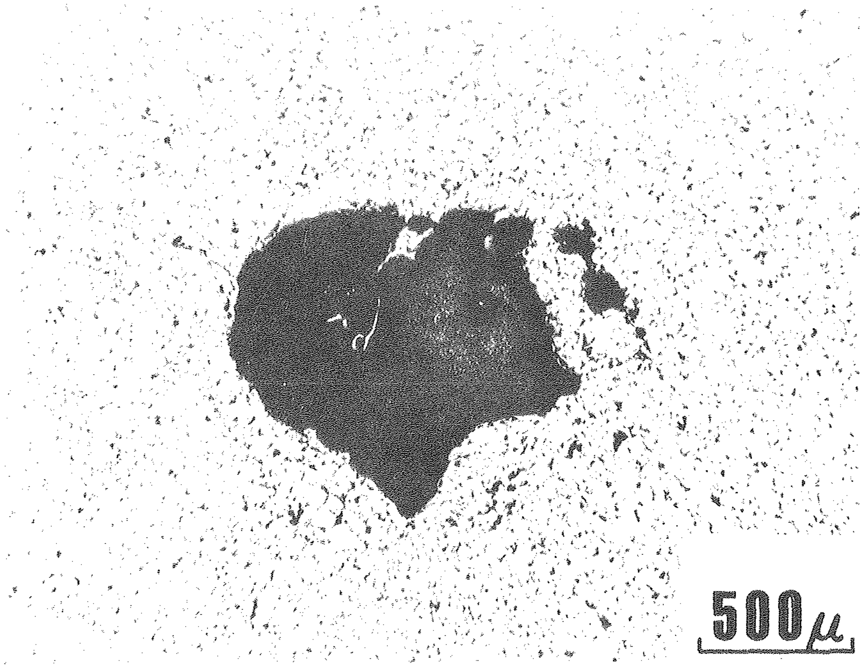

Fig. 31

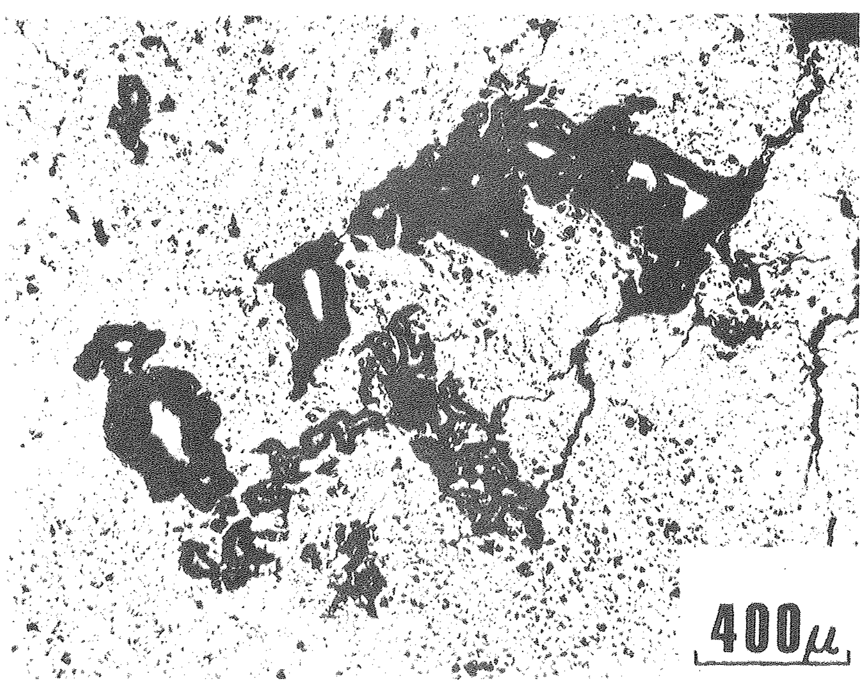

XBB 777-6300

Fig. 32